Oligogalacturonide Application Increases Resistance to Fusarium Head Blight in Durum Wheat

Valentina Bigini[1], Fabiano Sillo[2], Sarah Giulietti[1,3], Daniela Pontiggia[3,4], Luca Giovannini[2], Raffaella Balestrini[2*], and Daniel V. Savatin[1*]

[1]Department of Agriculture and Forest Sciences, University of Tuscia, Via S. Camillo de Lellis, 01100 Viterbo, Italy

[2]National Research Council, Institute for Sustainable Plant Protection, Strada delle Cacce 73, 10135, Torino, Italy

[3]Department of Biology and biotechnologies 'Charles Darwin', Sapienza University of Rome, P. le Aldo Moro 5, 00185 Rome, Italy

[4]Research Center for Applied Sciences to the safeguard of Environment and Cultural Heritage (CIABC), Sapienza University of Rome, P.le Aldo Moro, 5 00185 Rome, Italy

valentina.bigini@unitus.it (https://orcid.org/0000-0001-9415-3582)

fabiano.sillo@ipsp.cnr.it (https://orcid.org/0000-0002-1218-9985)

sarah.giulietti@unitus.it (http://orcid.org/0000-0003-0363-436X)

daniela.pontiggia@uniroma1.it (http://orcid.org/0000-0002-0980-107X)

luca.giovannini@ipsp.cnr.it (https://orcid.org/0000-0002-6528-5030)

raffaella.balestrini@ipsp.cnr.it (https://orcid.org/0000-0001-7958-7681)

daniel.davatin@unitus.it (https://orcid.org/0000-0002-2165-1369)

*Corresponding

raffaella.balestrini@ipsp.cnr.it

daniel.savatin@unitus.it

Highlight

The application of oligogalacturonides (OGs) directly enhanced the resistance of durum wheat plants against the phytopathogen *Fusarium graminearum*, highlighting their potential as a promising strategy in sustainable crop protection.

Abstract

Fusariosis causes substantial yield losses in wheat crop worldwide and compromises food safety because of the presence of toxins associated to fungal disease. Among the current approaches to crop protection, the use of elicitors able to activate natural defense mechanisms in plants represents a strategy gaining increasing attention. Several studies indicate that applications of plant cell wall-derived elicitors, such as oligogalacturonides (OGs) derived from partial degradation of pectin, induce local and systemic resistance against plant pathogens. The aim of this study was to establish the efficacy of OGs in protecting durum wheat, characterized by an extreme susceptibility to *Fusarium graminearum*. To evaluate the functionality of OGs, spikes and seedlings of *cv*. Svevo were inoculated with OGs, *F. graminearum* spores and a co-treatment of both. Results demonstrated that OGs are active elicitors of wheat defenses, triggering typical immune marker genes and determining regulation of fungal genes. Moreover, bioassays on spikes and transcriptomic analyses on seedlings showed that OGs can regulate relevant physiological processes in Svevo with dose-dependent specificity. Thus, the OG sensing system plays an important role in finetuning immune signaling pathways in durum wheat.

Keywords

Durum wheat, *Fusarium graminearum*, Oligogalacturonides, Immune Signaling, Transcriptomics, Cell Wall

Introduction

Nowadays, worldwide crop losses from phytopathogens range from 17% to 30% for major agricultural crops, undermining the urgent goal of a 70% increase required to satisfy the food demand, and directly affecting food quality and human health (Botticella et al., 2021; Savary et al., 2019). Fusarium Head Blight (FHB), or fusariosis, is a destructive fungal disease mainly caused by *Fusarium graminearum (Fg)* and can lead to a 50-70% loss of marketable grain (Alisaac and Mahlein, 2023). Besides reducing grain weight and quality during the infection, *Fusarium* species produce several trichothecene mycotoxins, including deoxynivalenol and nivalenol, which are toxic for humans and animals (Häggblom and Nordkvist, 2015), representing a significant hazard in the food chain (Magan and Aldred, 2007). Additionally, climate changes are predicted to positively impact on the frequency and severity of FHB epidemics (Jung et al., 2022).

Control strategies for fusariosis are still limited: in bread wheat, genetic variation for resistance to FHB is large and a multitude of resistance sources from "foreign" and "native" wheat germplasm are known (Steiner et al., 2017). Conversely, durum wheat is notorious for its high susceptibility to FHB (Miedaner et al., 2017) and breeding for FHB resistance is difficult due to the lack of resistance sources (Miedaner et al., 1997) as well as to difficulties in efficiently combining the numerous small-effect resistance quantitative trait *loci* (Steiner et al., 2019). Therefore, new, harmless, and sustainable control strategies for FHB disease management are urgently required. The exploitation of the plant innate immunity is needed considering that, if timely activated, it can efficiently contrast, and restrict plant infection by microorganisms. The innate immunity represents in fact the first step in defense against invaders and can be activated within a few minutes after sensing immunogenic signals derived both from pathogens and plant tissue damage (Abdul Malik et al., 2020). The faster pathogen detection occurs, the sooner proper immune responses are mounted by plants, with a consequent higher probability to restrict or block the tissue invasion. An active route for fungus entry is penetrating the epidermal cuticle and cell wall with short infection hyphae (Mary Wanjiru et al., 2002). As a surrounding barrier, the cell wall represents the first obstacle for the fungal entry. *Fg* secretes a broad spectrum of cell wall-degrading enzymes used to overcome the plant cell wall and to facilitate the assimilation of nutrients (Henrissat, 1991; Yang et al., 2012; Kubicek et al., 2014; Benedetti et al., 2019). Pectin degradation by fungal polygalacturonases favors the accumulation of oligomeric homogalacturonan degradation intermediates, *i.e.*, oligogalacturonides (OGs), recognized as danger signals by plant specific receptors and able to activate downstream immune responses (Ferrari et al., 2013; Savatin et al., 2014; De Lorenzo and Cervone, 2022). More than 40 years ago, phytoalexin accumulation in soybean cotyledons provided the first evidence that pectin fragments activate defensive responses (Hahn et al.,

1981). These fragments were later identified as oligomers of alpha-1,4-linked galacturonosyl residues (Nothnagel et al., 1983). OGs are nowadays probably the best characterized plant damage associated molecular patterns (DAMPs) and can elicit a wide range of defense responses in several plant species (Ferrari et al., 2013; Desaki et al., 2012; Pontiggia et al., 2020). An important aspect to be considered is that the OG different degree of polymerization (DP) determines their physiological properties and biological function. Different studies have demonstrated that long OGs (DP > 10) are the most effective in modulating immune signaling, while short OGs have little or no effect in Arabidopsis (Ferrari et al., 2007; Denoux et al., 2008). However, other studies have suggested that also short OGs (DP < 10) can impact plant defense (Simpson et al., 1998) and development (Miranda et al., 2007; Pontiggia et al, 2020). For instance, short OGs (DP4-6, DP2 and DP1-7) were shown to induce immune marker genes in potato and tomato and the synthesis of phytohormones in tobacco and tomato (Montesano et al., 2001; Simpson et al., 1998; Norman et al., 1999). Furthermore, Davidsson et al. (2017) investigated the role of trimers (DP3). Transcriptomic analysis of *Arabidopsis thaliana* exposed to such compounds suggested that DP3 may induce the expression of genes involved in the plant defense, even if gene expression induced by trimers was generally not as strong as that induced by long OGs. However, a few studies were made to study the effects of OGs in wheat plants (Randoux et al., 2010; Ochoa-Meza et al., 2021), none describing their role in resistance to fusariosis.

Over the years, one contentious issue has been whether *Fg* exhibits a biotrophic lifestyle during the initial stages of infection of floral tissues (Brown et al., 2010; Trail, 2009; Erayman et al., 2015; Chen et al., 2021). A detailed microscopic study of the *Fg* infection process in wheat heads found no indication of necrotrophy at the initial stages of infection, as the advancing *Fg* hyphae remained in the intercellular spaces of wheat rachis cells before subsequent intracellular growth, which presumably leads to subsequent cell death and necrosis (Brown et al., 2010). Therefore, *Fg* may be classified as a hemibiotrophic pathogen. Ding et al. (2011) demonstrated that resistance to *Fg* infection is associated with coordinated and ordered expression of diverse defense signaling pathways and altered secondary metabolism. Furthermore, Zhang et al. (2012) observed that the genes associated with the fungus non-symptomatic stage are involved in primary metabolic pathways, whereas transcripts corresponding to genes involved in cell wall degradation dominate the later growth stage of the infection process. Notably, the comparison of the transcriptomes of *Fg* feeding on living or dead tissues suggests that the fungus uses host signals to modulate the expression of several genes (Boedi et al., 2016). Some fungal genes are repressed by host signals (Boedi et al., 2016). On the other hand, host signal sensing is also required for the activation of DON biosynthesis. DON is a virulence factor in wheat, causing tissue necrosis and allowing the fungus spread into the rachis from florets in wheat (Jansen et al., 2005; Bian et al., 2021).

Numerous studies indicate that local application of cell wall-derived elicitors, such as OGs, induces broad-spectrum, long-lasting, and systemic resistance against pathogens in different plant species, such as *Arabidopsis*, rice, grapevine, and tomato (Ferrari et al., 2007; Aziz et al., 2004; Moscatiello et al., 2006; Gamir et al., 2021). The aim of this study was to investigate the role of OGs in durum wheat - *Fg* interaction. Data here reported clearly show that OGs are perceived as danger signals capable of inducing immune responses and resistance to fusariosis in durum wheat cotyledons and spikes. To facilitate the elucidation of molecular mechanisms regulating plant defense activation upon OG sensing, RNA sequencing was carried out to obtain a general view of the transcriptome in durum wheat seedlings inoculated with OGs at different concentrations (10 and 500 µg/ml), *Fg* spores or a co-treatment of both OGs and fungus spores. Chitosan (CHIT100 µg/ml) was used as a positive control in the experimental setup. The knowledge on the OG biology in durum wheat here generated will allow to shed light on the role of DAMP signaling in cereals and to open new perspectives on the application of molecular engineering approaches to strengthen plant immune responses against *Fg* and, possibly, other pathogenic microorganisms.

MATERIALS AND METHODS

Plant and fungal growth conditions

Plant material was prepared according to the protocol described in Jia et al. (2017). Wheat seeds *cv.* Svevo were rinsed with running water and then soaked overnight at 4°C in a 500 ml flask containing sterile water to help seeds to break dormancy and germinate faster. The imbibed seeds were placed in Petri dishes (90 mm diameter) containing 2 layers of sterile paper and germinated in the dark for 2 days at 25°C in a growth chamber. Germinated seeds were then transplanted to 24-well cell culture plates, one seed per well, and grown in the growth chamber for 1 day under controlled environment conditions at 25°C with a 18 h light/6 h dark photoperiod.

The fungal pathogen *Fg* strain 3827 was cultured at 25°C on potato dextrose agar (PDA) medium (AppliChem GmbH; Darmstadt, Germany). To induce macroconidia production, the fungus was cultured at 25°C on synthetic nutrient agar (SNA) medium (Urban et al., 2002) containing 0.1% KH2PO4, 0.1% KNO3, 0.1% MgSO4*7H2O, 0.05% KCl, 0.02% glucose, 0.02% sucrose, 2% bactoagar (Becton Dickinson; New Jersey, USA). Macroconidia were harvested from 90 mm SNA agar plates after 10 days of incubation by adding 1 ml sterile water and scraping off conidiospores with a spatula. Conidia concentration was estimated by Thoma chamber, adjusting the concentration to the proper concentration

for the infection assays. For long-term storage at -80°C, conidiospore suspensions were prepared to a density of 10^6 spores/ml in 10% glycerol.

In order to investigate the direct effect of OGs on *Fg* spore germination and mycelium growth, *Fg* spores (10^4 conidia) were placed in PDA plates containing different amounts (10, 500 µg/ml) of OGs. CHIT (2, 20, 100 µg/ml) was used as positive control. Mock control was also included. The plates were incubated in the dark for 5 days at 24°C. The mycelial growth was evaluated by measuring four fungal colony diameters from each plate by using the freely available ImageJ software (http://rsbweb.nih.gov/ij/). Data were obtained from three independent experiments, each one consisting of five replicates for each elicitor and concentration tested.

Oligogalacturonides were prepared according to the protocol described in Pontiggia et al. (2015). High molecular weight un-methylated polygalacturonic acid (PGA; Alfa Aesar) was solubilized in 100 ml of sodium acetate 50 mM, pH 5.0 to a concentration of 2% (w/v). The solution was digested for 180 min with 0.018 RGU of *A. niger* endoPG, and the enzyme was inactivated by boiling the digest at 100°C for 10 min in a water bath. After enzyme inactivation, the sample was diluted with 50 mM sodium acetate to a concentration of 0.5% PGA. To precipitate OGs, ethanol was added to the digest to a final concentration of 17% (v/v); the sample was incubated overnight at 4°C with shaking and then centrifuged for 30 min at 30000xg. OGs, recovered in the pellet, were re-dissolved in water, dialyzed against water in a dialysis tube with a molecular mass cut off (MWCO) of 1000 Da (Spectra/Por®), and lyophilized. OGs were analyzed by HPAEC-PAD with an ICS-6000 apparatus (Thermos Fischer) equipped with a CarboPac PA100 3 × 250 mm analytical column with a guard column (Thermo Fisher). A flow of 0.4 ml/min was used, and the temperature was kept at 35°C. The injected samples (10 µg) were separated using a gradient with 0.05 M NaOH (A) and 1 M Na-acetate in 0.05 M NaOH (B): 0–30 min from 20% B to 90% B,30–32 min at 90% B. Before injection of each sample, the column was equilibrated with 80% A and 20% B for 10 min. For MALDI–MS analysis, the matrix solution was prepared by dissolving 2,5-dihydroxybenzoic acid (DHB) in a solution of 70% acetonitrile with 0.1% trifluoroacetic acid to a final concentration of 20 mg/ml. The samples (5 mg/ml in water) were pre-treated for 10 min with BioRex MSZ501 cation exchange resin beads (BIO-RAD) and then prepared as dried-droplets by spotting 1 µl of matrix solution first on the stainless steel MALDI target and adding 1 µl of sample solution immediately afterward. MALDI–TOF–MS measurements were performed on an UltrafleXtreme TOF/TOF mass spectrometer equipped with a reflector and controlled by the FlexControl 2.2 software package (Bruker Daltonics).

Shrimp shell chitosan (molecular weight 190-375 kDa, degree of deacetylation ≥75 %, CAS number 9012-76-4, CAT number 417963) was purchased from Merck (Darmstadt, Germany). Chitosan stock solution (10 mg/ml) was prepared by dissolving the required amount of chitosan powder in 1M acetic

acid. The stock solution was autoclaved and subsequently added to sterile, distilled water to obtain desired final chitosan concentrations.

F. graminearum infection assay in wheat spikes and seedlings

Wheat seeds *cv*. Svevo were surface sterilized with 75% (v/v) ethanol for 2 min, 40% (v/v) sodium hypochlorite for 15 minutes and then rinsed thoroughly in sterile water. Seed germination was performed in Petri dishes (90 mm diameter) containing 2 layers of sterile paper. When seminal roots and the hypocotyls emerged, around 10 days post-germination, seedlings were transferred in jiffy pots with soil, and vernalized at 4°C for 1 month. Afterwards, plants were grown in a climatic chamber at 18 to 23°C with a 18h light/6h dark photoperiod. When plants presented the second/third leaf, they were two by two transferred in 14x14 cm pots. PDA medium (AppliChem GmbH; Darmstadt, Germany) was used for the growth and maintenance of *Fg* strain 3827, and SNA medium was used to promote sporulation, as described previously.

Inoculation assays on wheat spikes *cv*. Svevo were conducted as reported by Makandar et al. (2012). At anthesis stage, inoculation of wheat plants was performed by single-spikelet inoculation. Briefly, the glumes of two opposite central florets of a wheat head were inoculated with OGs (500 µg/ml), *Fg* spores (2 x 10^4 conidia) and a co-treatment of both OGs and fungus spores. Sterile water was used as mock treatment and CHIT (100 µg/ml) as a positive control in the experimental setup. High humidity conditions were maintained for 3 days by covering the inoculated spikes with a plastic bag. Over time, the fungal infection spread out to the other spikelets within each spike. FHB disease symptoms were assessed by counting the number of visually diseased spikelets at different days post-infection (dpi) and by relating them to the total number of spikelets of the respective head, resulting in a percentage of symptomatic spikelets. The final count was taken at 21 dpi. For each experiment, at least 15 plants for treatment were used.

To investigate the capability of OGs to induce immune responses and resistance systemically, we germinated and grew wheat seedlings on half MS containing 10, 100, 500 µg/ml OGs and 2, 20, 100 µg/ml CHIT for three days before inoculating Fusarium spores in coleoptiles as reported by Jia et al. (2017). Briefly, the top 1-2 mm of three-day-old wheat coleoptiles were cut off and inoculated with *Fg* spores (2 x 10^3 conidia). Sterile water was used as mock treatment. The inoculated seedlings were grown in a climatic chamber for 7 days under controlled environment conditions at 24°C with a 18 h light/6 h dark photoperiod and 95% relative humidity. Lesion size on coleoptiles of inoculated wheat seedlings was measured at different dpi. The final measurement was taken at 7 dpi. The longitudinal length of brown lesions on wheat

coleoptiles was measured as the lesion size at the indicated time by using ImageJ software (http://rsbweb.nih.gov/ij/). For each experiment, at least 15 seedlings for treatment were used.

Quantification of fungal biomass in durum wheat seedlings and spikes

Genomic DNA from different inoculated seedlings and spikes was extracted with Nucleospin Plant II kit (Macherey-Nagel, Oensingen, Switzerland) according to manufacturer's instructions. After a quality and quantity check, a quantitative real-time polymerase chain reaction (qPCR) was performed by using a CFX96 Real-Time System (Biorad, Hercules, CA, USA) and amplifying 50 ng of gDNA in a 20 µl reaction mixture containing 1X SsoAdvanced Universal SYBR green Supermix (Biorad, Hercules, CA, USA) and 0.5 µM of each primer. qPCR data analysis was done by using LinRegPCR software. The DNA content of the *Fg* β-tubulin gene (*Fg β-tubulin*), relative to the wheat actin gene (*TdACTIN*), was determined in wheat seedlings (7 dpi) and spikes (6, 24 and 48 hours post infection - hpi) inoculated with *Fg* spores and the co-treatment of both OGs and fungus spores. Results were determined by using the Pfaffl method (Pfaffl, 2001) and expressed in arbitrary units. Primer sequences are shown in Supplementary Table S1.

Elicitor treatments in durum wheat seedlings

Following sterilization (see above) seeds were washed three times with sterile water and placed in Petri dishes (90 mm diameter) containing sterile paper. Three days after germination, seedlings were transferred in sterile culture tubes containing half-strength Murashige and Skoog medium supplemented with sucrose 0.5% (w/v) (Sigma-Aldrich, Burlington, MA, USA) and solidified with agar 0.8% (w/v) (Duchefa Biochemie, Haarlem, The Netherlands) at pH 5.8, in the absence or presence of different concentrations (10, 500 µg/ml) of purified OGs. Chitosan (2, 20, 100 µg/ml) was used as known compound affecting wheat growth in the experimental setup (Liu et al., 2021). After seven days in a growth chamber at 24°C with a 16 h light/8 h dark photoperiod, fresh weight, root length and first leaf length were measured for each seedling. The root length and the first leaf length of all plantlets were measured by using the freely available ImageJ software (http://rsbweb.nih.gov/ij/).

RNA sequencing

Three-day-old wheat seedlings were inoculated with OGs (10 and 500 µg/ml), *Fusarium graminearum* spores (2 x 10^3 conidia) and a co-treatment of both OGs and fungus spores. Sterile water was used as mock treatment (control), and CHIT (100 µg/ml), whose priming ability has already been demonstrated (Deshaies et al., 2022), was also included in the experimental setup. Three biological

replicates, for each condition, were selected at 48 hpi: Mock (Mock), plants elicited with chitosan (100 µg/ml – CHIT100), plants elicited with OGs (10 µg/ml – OG+10, and 500 µg/ml – OG+500), plants inoculated with *Fg*, plants inoculated with *Fg* and cotreated with elicitor compounds (*Fg*+CHIT100, *Fg*+OG10, *Fg*+OG500). For each sample, fresh plant material (approximately 100 mg) was frozen by using liquid nitrogen, ground in 2 ml tubes by using steel beads (diameter 0.4 mm) and homogenized through a TissueLyser II (Qiagen, Valencia, CA, USA). Total RNA was isolated by using a CTAB-based lysis buffer following the 'pine tree method' (Chang et al. 1993). The RNA pellet was resuspended in DEPC-treated water and quality of the extracted RNA was determined by using a Nanodrop 2000 spectrophotometer (Thermo Fisher Scientific, Waltham, MA, USA). Library preparation and RNA sequencing were performed by GENARTIS s.r.l. laboratories (Verona, Italy). In total, 24 Illumina RNA-seq libraries were generated using the TruSeq stranded mRNA ligation kit (Illumina) from 700 ng of RNA samples, after poly(A) capture and according to manufacturer's instructions. Using the Agilent 4150 Tape station (Agilent), capillary electrophoretic analysis was carried out to measure the quality and size of the RNAseq libraries. Libraries were quantified by real-time PCR against a standard curve with the KAPA Library Quantification Kit (KapaBiosystems, Wilmington, MA, USA) and sequenced with Illumina technology in 150PE mode on a Novaseq6000 sequencer. Raw reads from RNA-seq were submitted to NCBI Sequence Read Archive (Bioproject PRJNA977839).

RNA-Seq Data Analysis and Differential Gene Expression Quantification

The RNA-sequencing obtained reads were aligned to the transcriptome of durum wheat (Maccaferri et al., 2019) available at https://plants.ensembl.org/ using the Salmon software v1.4.0 (Patro et al., 2017). Salmon uses a quasi-mapping approach to align the reads, which allows for more sensitive and accurate alignment compared to traditional methods. This software estimates the relative abundance of different transcripts as transcripts per million (TPM), a normalization method computed considering the library size, number of reads and the effective length of the transcript (Patro et al., 2017). Raw read counts and TPM data were generated from each Salmon output file, by combining isoform counts to obtain counts at gene level. The outputs including transcript lengths, count of aligned reads and abundance estimates were imported in DESeq2 by using the R package tximport v1.22.0 (Soneson et al., 2015) using the length ScaledTPM method. Principal components analysis (PCA) was performed on normalized gene counts (regularized log transformation of normalized data) using DESeq2 package v1.34.0 (Love et al., 2014). The data were used to identify differentially expressed genes (DEGs) using the DESeq2 package v1.34.0 (Love et al., 2014). The variance on reads count was calculated based on the three biological replicates per condition by applying a negative binomial distribution to model the count data and identify genes with

significant changes in expression between the different conditions. The DEG identification was performed after normalization of the count data and correction for multiple testing, both accounted by DESeq2, through Wald test, and using mock condition (water treatment) as control. Variance on reads count was calculated based on the three biological replicates per condition. During DESeq2 analysis, shrinkage estimation of effect size (LFC estimates) was used, in order to generate more accurate Log2 Fold Change (Log2FC) estimates and taking into account variability among replicates. A threshold of adjusted p <0.05 were used to identify DEGs. A cut-off of the p-adjusted value ≤ 0.05 was used to classify a gene as differentially expressed (DEG) in comparison with the control. Both the identified DEGs and all transcripts of the Svevo transcriptome were annotated through Blast2GO v5.2.5 (Conesa et al., 2005) to obtain an updated functional annotation and to assign their associated Gene Ontology (GO) terms. The identified DEGs were then analysed for functional enrichment using Blast2GO to reveal the biological processes, pathways, or other functional categories that are enriched among the DEGs. To perform GO enrichment analysis and to provide a summary of the functions and pathways associated to the obtained sets of DEGs, ShinyGO v0.77 online tool was used (Ge et al., 2020). In addition, reads obtained from samples inoculated with Fg, as well as from samples inoculated and co-treated with both OGs and CHIT100, showing no alignment on plant transcriptome, were aligned using Salmon on *F. graminearum* transcriptome strain PH-1 (Cuomo et al., 2007) available at MycoCosm web portal by Joint Genome Institute (JGI; https://mycocosm.jgi.doe.gov/Fusgr1/Fusgr1.home.html). The same pipeline used for plant via txtimport v1.22.0 was used for detecting reads putatively belonging to the fungus. By using *Fg*-inoculated samples without OGs as reference, DESeq2 v1.34.0 was used to assess fungal DEGs (threshold of adjusted p <0.05).

Validation of RNA-seq through RT-qPCR on selected genes

The differential expression of 11 selected DEGs obtained from RNA-seq analysis was validated through RT-qPCR. The RNA samples from the three biological replicates for each condition assessed through RNA-seq (for a total of 24 samples) were treated with TURBO DNA-free™ Kit (Thermo Fisher Scientific, MA, USA) to remove genomic DNA, whose absence was verified by PCR using primers designed on the reference gene coding for GAPDH (GenBank accession: EU022331.1). The RNA was then converted into cDNA by using the SuperScript™ II Reverse Transcriptase kit (Thermo Fisher Scientific), starting from 1 µg of RNA per sample. The RT-qPCR reactions were performed in the ConnectTM Real-Time PCR Detection System (Bio-Rad Laboratories, CA, USA), using the Power SYBR Green PCR Master Mix (Bio-Rad Laboratories). The primers used for the amplification (Supplemtary Table S1) were designed

on the coding sequences of the selected genes using the online software Primer3 (https://primer3.ut.ee/). The obtained cDNA was diluted 1:3 to be used as a template for the reactions, and two technical replicates were used for each of the three biological ones. Each RT-qPCR reaction was performed on a total volume of 10 µl, containing 1 µl cDNA, 15 µl Power SYBR Green PCR Master Mix (Bio-Rad Laboratories) and 0.2 µl of each primer (final concentration of 200 nM), using a 96-well plate. The following PCR protocol, which includes the calculation of the melting curve, was used: 95°C for 30 seconds, 40 cycles of 95°C for 10 seconds and 60°C for 30 seconds, ramp from 65°C to 95°C with a temperature increment of 0.5 °C and a read plate every 5 seconds. For the normalization of gene expression data, two reference genes, *i.e.*, one coding for GAPDH and one for Actin (GenBank accession: AB181991.1), were used. The $2^{-\Delta\Delta CT}$, where ΔΔCt represents the ΔCt sample − ΔCt control (Mock), was used to calculate the fold change for each tested gene (Livak et al., 2001) and the results obtained by RT-qPCR and RNA-seq were compared using Pearson correlation coefficients.

Statistical Analysis

Data were analyzed with Student's t-test or ANOVA by using the SYSTAT12 software (Systat Software Incorporated, San Jose, CA, USA). When significant F values were observed ($p < 0.05$), a pairwise analysis was carried out by the Tukey Honestly Significant Difference test (Tukey test).

RESULTS

OGs trigger resistance to *F. graminearum* in durum wheat spikes

To evaluate the functionality of OGs as elicitors of immunity and their ability to restrict phytopathogen fungal growth in durum wheat spikes at the anthesis stage, two opposite central florets of a wheat head were inoculated with OGs (500 µg/ml), *Fg* spores (2 x 10^4 conidia) and a co-treatment of both OGs and fungus spores. Before the treatment, degree of polymerization of the corresponding oligomers was characterized by HPAEC-PAD and MALDI-TOF analyses (Supplementary Figure S1). Sterile water was used as mock treatment and CHIT (100 µg/ml) as a positive control in the experimental setup. We observed that symptom progression was slower in spikes co-treated with OGs and fungus spores than in spikes inoculated with the fungus alone. The maximal reduction of 25% in symptom severity was detected between 7 and 13 dpi (Figure 1A). At this infection stage, several OG-cotreated inoculated spikelets showed a temporary block of the infection. The spikes cotreated with CHIT and *Fg* did not show symptoms of the

fungal disease (Figure 1A), likely because of the inhibitory effect of CHIT on *Fg* spore germination and hyphal development (Deshaies et al., 2022). The fungal abundance in the different treatments was monitored by quantifying the DNA accumulation through qPCR, amplifying the *Fg β-tubulin* gene, and resulted significantly lower in spikes of plants cotreated with fungus and elicitors. In presence of the OG-cotreatment, the fungal DNA amount was 84.6%, 61.5% and 84.4% compared to spikes inoculated with the fungus alone at 6, 24 and 48 hpi, respectively (Figure 1B). Interestingly, results showed that, compared to the *Fg* control condition, in the CHIT and *Fg* co-treatments the fungal amount was only 4.6%. As shown in Figure 1C, at 10 dpi the severity of the symptoms is particularly evident in plants inoculated with the fungus alone, displaying 100% of the spikelets infected. On the contrary, spikes cotreated with OGs showed a considerably lower severity of the disease at this time point of the infection.

Impact of OGs on wheat agronomical and growth parameters

After verifying that OGs and CHIT can limit the infection spread of *Fg*, we evaluated the impact of the elicitors on important wheat agronomical and growth parameters after infection. The number of seeds per spike, the number of seeds per spikelet, the primary spike weight, the weight of seeds per spike, the weight of 1000 seeds and the yield loss were considered for analyses (Figure 2). In the *Fg*-inoculated plants, significantly lower yield values were observed for all the parameters considered. The number of seeds per spike and per spikelet were inhibited by 77.6% and 76.9%, respectively, compared to untreated plants (Figures 2A-B). Moreover, results showed an inhibition of the primary spike weight, the weight of seeds per spike and the weight of 1000 seeds by 77.3%, 95.1% and 73.8%, respectively (Figures 2C-E). Interestingly, no significant differences were observed compared to mock condition in plants cotreated with CHIT and the fungus.

In the presence of OG cotreatments, higher yield values were observed compared to *Fg*-inoculated plants. The inhibition percentages of the number of seeds per spike and per spikelet were 35.3% and 29.2%, respectively, compared to untreated plants (Figure 2A-B). For the primary spike weight, the weight of seeds per spike and the weight of 1000 seeds, a significant reduction of 36.6%, 38.9% and 48.6%, respectively, was observed (Figure 2C-E). Therefore, OGs limit the infection spread of *Fg* as well as the yield loss associated to fungal disease. The loss in production was then calculated and expressed as percentage (Figure 2F). *Fg*-inoculated plants displayed a production loss of 79.7%, while OG-cotreated plants exhibited a yield reduction of only 28.3% compared to the mock condition. No significant differences were observed between CHIT-cotreated and untreated plants.

The quality and the filling of kernels were also evaluated, considering the length and the width of wheat seeds, after *Fg* infection. As shown in Figure 3A-B, OG and CHIT treatments did not affect wheat seed length and width. On the contrary, the fungus *Fg* negatively impacted on both considered parameters by compromising the good filling of kernels and causing their shriveling.

Seeds derived from *Fg*-inoculated spikes displayed an inhibition of seed length and width of 33,4% and 43,75%, respectively, compared to untreated condition. No significant differences in seeds derived from CHIT-cotreated plants were observed compared to mock condition. Moreover, we observed that in the presence of OG-cotreatment, seeds displayed a reduced shriveling (Figure 3C) and an inhibition of length and width of only 6.5% and 25%, respectively (Figure 3A-B).

OGs trigger resistance to *F. graminearum* in durum wheat seedlings

The OG-related effects on plant morphological parameters were assessed by growing durum wheat seedlings, *cv*. Svevo, on MS medium in the absence or presence of different concentrations (10, 500 µg/ml) of purified OGs for 7 days. CHIT (2, 20,100 µg/ml) was used as a positive control (Liu et al., 2021). None of the OG treatments altered fresh weight, root length and first leaf length. Conversely, CHIT strongly inhibited all growth-related parameters considered in a dose-dependent manner (Figure 4A-C). Indeed, in the presence of CHIT 100 µg/ml, seedling fresh weight, root length and first leaf length were inhibited by 57.4%, 83.2% and 29,7%, respectively.

To evaluate the functionality of OGs as elicitors of immunity and their ability to restrict phytopathogen fungal growth also in durum wheat coleoptiles, three-day-old seedlings were inoculated either with OGs at different concentrations (10, 100, 500 µg/ml), *Fg* spores (2 x 10^3 conidia) or a co-treatment of both OGs and fungus spores. Sterile water was used as mock treatment and CHIT (2, 20, 100 µg/ml) as a positive control in the experimental setup. In the presence of co-treatments with both OGs or CHIT and the spores, disease lesion size and fungal accumulation, evaluated at different dpi, were significantly lower compared to seedlings treated with the fungus spores only (Figure 5A-C). At 7 dpi, seedlings co-treated with OG 10, 100 and 500 µg/ml showed a significant disease lesion size reduction of 14.8%, 41.8% and 45.3%, respectively. Seedlings inoculated with both CHIT and *Fg* displayed a reduction of 60.6% compared to seedlings treated with the fungus alone. It is worth noting that OGs triggered resistance to FHB in a dose-dependent manner, with the higher OG concentration used displaying the greater reduction in symptoms as well as in fungal accumulation. Indeed, in the presence of OG 10, 100 and 500 µg/ml, the fungal amount was decreased by 30,4%, 35,7% and 58,6% compared to seedlings treated

with the fungus alone, whereas cotreatment with CHIT and *Fg* restricted the fungal amount by 84% (Figure 5B).

To evaluate possible OG-dependent direct effects on fungal germination and/or growth we inoculated *Fg* spores in PDA plates containing different amounts (10, 500 µg/ml) of OGs. CHIT (2, 20, 100 µg/ml) was used as positive control. Measurements of the fungal radial growth showed an inhibitory effect of both pectin fragment amounts on Fusarium hyphae growth, similarly to what detected in CHIT containing plates (Supplementary Figure S2).

To ascertain the OG capability of activating systemic immune responses capable of restricting Fusarium colonization of wheat tissues, we germinated and grew wheat seedlings on half MS containing 10, 100, 500 µg/ml OGs for three days before inoculating *Fg* spores (2 x 10^3 conidia) in coleoptiles. As in the case of CHIT (2, 20, 100 µg/ml), used as control, seedlings treated with all doses of OGs considered were able to induce higher resistance to *Fg* (Figure 5A-D).

Transcriptome changes in elicited durum wheat seedlings infected with *F. graminearum*

Given the high similarity between the results obtained in spikes and seedlings infected with *Fg*, and to obtain a higher grade of reproducibility, the protocol published by Jia et al. (2017) for large-scale analyses has been adopted. RNAseq was carried out to obtain a general view of the transcriptome in durum wheat seedlings inoculated with OGs at different concentrations (10 and 500 µg/ml), *Fg* spores (2 x 10^3 conidia) or a cotreatment of both OGs and fungal spores for 48 hours. Sterile water was used as mock treatment (control) and CHIT (100 µg/ml) as a well-established priming agent in the experimental setup.

Sequencing of RNA samples produced an average of 36,994,174 reads per sample (ranging from 24,463,053 to 55,619,350; Supplementary Table S2). Reads mapped to the durum wheat transcriptome using *Salmon* resulted in an average mapping rate of 78.67% (ranging from 67.26% to 88.34%). Total wheat read counts are reported in Supplementary Table S3. The data distribution is evident by observing results from principal component analysis (PCA). The PCA of count data showed that RNA samples of *Fg* inoculated plants clustered far from the uninoculated ones, except for samples of plants inoculated with *Fg*+CHIT100 (Supplementary Figure S3A), that grouped into between the two groups. A limited variability was observed for samples of uninoculated plants (Supplementary Figure S3B), while biological replicates of plants affected by the pathogen resulted slightly dispersed, considering *Fg* and *Fg*+OG treatments (Supplementary Figure S3C). Conversely, *Fg*+CHIT100 replicates grouped separately (Supplementary Figure S3C). A total of 4345 genes (out of 66073 *T. turgidum* subsp. *durum* total genes) were found to be

differentially regulated in all samples. The differentially expressed genes (DEGs) compared to the control condition (mock) and identified in the diversely treated wheat coleoptiles are reported in Tables S4-S12.

Considering the total up- and down-regulated genes (Supplementary Table S4), the treatment with most up-regulated genes resulted *Fg*+OG500 (2728 out of 2906 regulated genes) while the treatment with most down-regulated genes was *Fg* (494 out of 3214 regulated genes). As conceivable, the expression of a high number of genes was reprogrammed by the presence of the pathogenic fungus (6A-C, Supplementary Table S4). The gene expression patterns of treatments without *Fg*, depicted in Supplementary Figure S4, revealed a modest transcriptional remodeling in plants subjected to elicitors. Notably, the treatment involving CHIT100 exhibited dissimilar gene expression patterns compared to the two OG treatments. Additionally, while there was some overlap in the DEGs between the two OG treatments, distinct transcriptomic profiles were evident. Looking at the three immune elicitor treatments (OG10, OG500 and CHIT100), 84 genes were found to be exclusively regulated in OG10, 84 in OG500 and 133 in CHIT100 (Supplementary Figure S4) compared to mock condition. A total of 13 DEGs were shared among the three different treatments on not inoculated plants (Supplementary Table S13).

The heatmap in Figure 6 reports the whole transcriptomic reprogramming in seedlings inoculated with *Fg* compared to the mock control condition, with and without immune elicitors, and shows that *Fg* and *Fg*+OG500 treatments exhibited similar patterns in terms of DEGs. On the other hand, the treatment *Fg*+OG10 appeared to have a distinct pattern compared to the other treatments, likely hinting the activation of distinct signaling regulators and/or mechanisms. Particularly, *Fg*+OG10 is the treatment with the highest number of exclusive up-regulated genes (360 *vs* 220 in *Fg* as well as in *Fg*+OG500, and 78 in CHIT100) (Figure 6). Moreover, *Fg*+CHIT100 showed a reduced number of DEGs compared to the other treatments. This might be due to the inhibitory effect of chitosan on Fusarium spore germination and to a consequent minor amount of plant cells challenged. In the presence of the phytopathogen fungus, only six genes were found to be commonly regulated between the elicitor co-treatments, including a hexokinase (TRITD1Bv1G065190), an auxin responsive gene SAUR 36-like (TRITD5Av1G189370), a transcription factor WRKY19-like (TRITD2Av1G050640), a mannose/glucose-specific lectin-like protein (TRITD4Av1G248450), a photosystem II phosphoprotein (TRITD1Bv1G023480), and a exocyst complex component EXO70B1 (TRITD0Uv1G091020) (Figure 6, Supplementary Table S14).

Infection marker genes, such as pathogenesis-related (*PR*) genes (Supplementary Table S15), were up-regulated in all the *Fg* treated samples. The expression of 12 *PR1* genes, among the 24 paralogs in durum wheat genome, was differently regulated in the different treatments, with some differences among them. Particularly, only one gene (TRITD5Bv1G112400) resulted significantly up-regulated in *Fg*+CHIT100

(Log2FC = 5.69), while all the *PR1* set was regulated with a Log2FC average of 7.40, 5.22 and 7.61 in *Fg*, *Fg*+OG10 and *Fg*+OG500, respectively (Supplementary Table S15). Significant differences among average expression values of *PR1* genes in the four different treatments (*Fg*, *Fg*+OG10, *Fg*+OG500 and *Fg*+CHIT100) were detected. *PR1* expression was significantly higher in *Fg*, *Fg*+OG500 and *Fg*+OG10 compared to *Fg*+CHIT100 ($p < 0.0001$), and in *Fg*+OG500 compared to *Fg*+OG10 ($p = 0.040$). Although no significant differences were detected between *Fg* and *Fg*+OG500 expression values ($p = 0.9944$), *PR1* expression in *Fg*+OG500 was slightly higher compared to *Fg* (7.61 *vs* 7.40). Considering the down-regulated genes, no gene was commonly down-regulated between *Fg*+OG10 and *Fg*+OG500, whereas the highest number of exclusive down-regulated genes were found in *Fg* (318) followed by *Fg*+OG10 (184), *Fg*+OG500 (75) and *Fg*+CHIT100 (57) (Figure 6C).

Shared and exclusive DEGs were found among *Fg*, *Fg*+OG500, displaying the highest OG-induced resistance in the pathogenicity assays, and OG500 alone (Figure 7). Among the 113 DEGs in OG500 (Supplementary Table S4), 47 were exclusive, while 62 were in common with *Fg* and *Fg*+OG500, although with a different expression level (59 up-regulated in the three treatments and 3 down-regulated in OG500 and up-regulated in *Fg* and *Fg*+OG500; Supplementary Table S2). Comparing the expression of these genes in OG10 and *Fg*+OG10, it was evident that a diverse regulation occurred (Supplementary Figure S5), suggesting that a threshold effect due to the different OG concentrations could explain the difference in transcriptome profile. Several commonly regulated DEGs in these conditions encode for transcription factors belonging to diverse groups as well as for defense-related proteins (Figure 8). Indeed, in agreement with Kazan & Gardiner (2018), the presence of *Fg* triggered the expression of genes involved in signaling and defense, cell wall remodeling, phenylpropanoid/lignin metabolism (*e.g.*, endoglucanases, laccases), transport (*e.g.*, ABC transporters), chitinases and glucan endo-1,3-beta-glucosidases (1,3-glucanases). Although several genes regulated in response to *Fg* infection showed a similar trend in both OG treatments, 295 and 544 genes were only regulated in *Fg*+OG10 or *Fg*+OG500, respectively, and others presented a diverse regulation in *Fg*+OG10 and *Fg*+OG500 (Figure 6, Supplementary Table S11). The top five genes found to be up-regulated only after the *Fg*+OG500 treatment, encode for a probable LRR receptor-like serine/threonine-protein kinase (Log2FC = 7.39; TRITD0Uv1G107190), a scopoletin glucosyltransferase-like (Log2FC = 6.91; TRITD2Av1G260470), a PLAT domain-containing protein 3 (Log2FC = 6.56; TRITD2Av1G287330), a peroxidase 2-like (Log2FC = 6.37; TRITD0Uv1G142450), and a glucan endo-1,3-beta-glucosidase GII-like (Log2FC = 6.29; TRITD3Bv1G259660). Moreover, two putative glycerol-3-phosphate transporter 1 (TRITD2Av1G242680 and TRITD2Bv1G203230), a known mobile regulator of systemic acquired resistance (Chanda et al., 2011), were up-regulated in *Fg*+OG500. Fungal cell wall degrading enzymes, such as chitinases, were also found to be up-regulated after the pathogen infection in

the presence of the OG treatments (Supplementary Table S12). One chitinase encoding gene (TRITD7Av1G248080) resulted to be up regulated in OG10 and OG500 treatments in the absence of the pathogen as well. Gene expression data obtained by RT-qPCR analysis of eleven selected DEGs showed a significant degree of correlation with data obtained with RNA-seq analysis (R2: 0.711, *p*-value: 2.503^{e-14}; Supplementary Figure S6 and Supplementary Table S16).

GO enrichment analysis

To have an overview of the regulation of the main metabolic processes and signaling pathways involved in the different comparisons, we conducted GO enrichment analysis.

Differentially expressed transcripts were grouped in functional classes, based on the specific biological process in which they are involved (Tables S17; Figures 8 and 9). Relevant terms found in OG10 transcriptome are "Cellular oxidant detoxification" and "Detoxification" (Figure 8A), whereas, in OG500 different defense related processes were identified such as "Lignin metabolic process", "Chitin catabolic process", "L−phenylalanine metabolic process" (Figure 8B). Results showed the presence in CHIT100 of different significant terms (FDR value < 0.05) including those related to detoxification and amino acid metabolism (Figure 8C). Significant GO terms found for transcripts in *Fg* treated samples included chitin catabolism, phosphorylation, defense, response to oxidative stress, amino acid metabolism (Figure 9A). Conversely, the OG10 co-treatment with the fungus (*Fg*+OG10) led to transcript enrichment mainly related to the "Glutathione metabolic process", one of the most significant terms also identified in *Fg*+OG500 samples (Figure 9B-C) together with "Cell wall catabolic process". As regards *Fg*+CHIT100, results showed the presence of different terms related to sulphur and amino acid metabolism, as in the case of CHIT100 (Figure 9D).

Transcriptome reprogramming by immunogenic signals in durum wheat seedlings

Considering the effects of the OG10, OG500 and CHIT100 treatments in uninfected plants, twelve genes have been found to be commonly up regulated (Supplementary Figure S4 and Supplementary Table S13), including genes previously reported to be involved in plant resistance to biotic stress in cereals, such as a *CASP-like protein*, 2 probable linoleate *9S-lypoxygenases 5* and *Bowman-Birk type trypsin inhibitor like* (Bhat et al., 2019). Other up-regulated genes were a *thaumatin-like protein* (TRITD6Bv1G225300), also found among the up-regulated genes in *Fg* treatment, followed by an ethylene-responsive transcription factor *ERF109-like* (TRITD1Bv1G202640) and a probable calcium-binding protein *CML25/26*

(TRITD4Av1G142800). Nevertheless, the two OG treatments exhibited dissimilar gene expression patterns compared to CHIT100 and, importantly, distinct transcriptomic profiles were also evident between treatments with OG10 and OG500 (Supplementary Figure S4). Indeed, 65 genes were found to be exclusively regulated in OG10, 71 in OG500 and 52 in CHIT100 (Supplementary Figure S4B). The most up-regulated gene in all the treatments resulted a *peroxidase 5 like* gene (TRITD0Uv1G116360), with the only exception of OG500 treatment, although a high variability has been observed among the biological replicates. Variability among biological replicate read counts of this gene may indicated that the observed difference can be influenced by technical and biological variation of the experiment. However, since LFC effect size estimator was used during DESeq2 analysis, and *p*-adjusted value is lower than the threshold ($p < 0.05$), the difference in expression can be the result of a true biological difference. Additionally, no reads corresponding to this transcript have been found in OG500 treatment in any replicates (Supplementary Table S3). An individual variability has been observed for several transcripts suggesting that expression for these genes might be very specific in timing and tissue localization. Despite the standardization in OG application and infection procedure, a seedling variability in the individual response might occur as already reported by Sorrentino et al. (2021).

Among the 71 exclusive up-regulated genes identified in OG500-treated tissues (padj < 0.05), several genes are involved in signaling and plant response to biotic stresses. Particularly, genes coding for a putative *polyamine oxidase-like* (Log2FC = 3.087; TRITD7Av1G204550), a *homeobox-leucine zipper* protein (Log2FC = 2.86; TRITD2Bv1G191820), a *mannose/glucose-specific lectin-like* (Log2FC = 2.87; TRITD4Av1G248390), two *GDSL esterase/lipase* proteins (Log2FC = 2.67; TRITD0Uv1G053990; Log2FC = 0.72; TRITD4Bv1G060640), a *dirigent protein* (Log2FC = 2.29; TRITD0Uv1G010390), an auxin-responsive protein *SAUR36-like* (Log2FC = TRITD5Av1G189140), a probable *apyrase* (Log2FC = 1.17; TRITD4Bv1G199760), a *germin-like protein* (Log2FC = 1.12; TRITD6Bv1G216490), a *NDR1/HIN1-like* protein (Log2FC = 0.76; TRITD3Bv1G120400), and a non-specific *lipid-transfer protein* (Log2FC = 0.72; TRITD2Bv1G226450). Moreover, genes coding for serine/threonine-protein kinases (TRITD0Uv1G123990, TRITD1Av1G199560, TRITD2Av1G294740) were specifically and significantly down-regulated in addition to a putative class II *heat shock protein* (TRITD3Bv1G044290), a *calmodulin-binding transcription factor activator* (TRITD2Bv1G141170), a transcription factor *VOZ-1 like* (TRITD1Bv1G186320) and a *3-hydroxyacyl-CoA dehydratase* gene (TRITD3Bv1G024940).

OG-dependent regulation of genes putatively involved in immune signaling and plant cell wall remodeling in durum wheat seedlings

Homologue genes of known important modulators of immune responses in plants have been identified as DEGs through the transcriptomic analyses. Intriguingly, genes potentially involved in the OG sensing and homeostasis, such as wall-associated receptor kinases (Wan et al., 2021), and members of Berberine-Bridge Enzyme-like (BBE-l) family (Pontiggia et al., 2020; Locci et al., 2019; Benedetti et al., 2018), were up-regulated (28 and 5 genes, respectively) during the infection, except in the *Fg*+CHIT100 cotreatment. Among the genes coding for the wall-associated receptor kinases, it is worth noting the presence of three genes exclusively regulated by OG500, *i.e.*, TRITD2Av1G016690, which resulted to be down-regulated in *Fg*+OG500 (Log2FC =-4.81), and TRITD5Bv1G188610 and TRITD6Bv1G224850, which conversely were up-regulated in the same condition (Log2FC = 1.05 and 5.76, respectively). Additionally, five genes belonging to the BBE-l family were differentially expressed in *Fg*, *Fg*+OG10 and *Fg*+OG500 treated seedlings compared to mock control condition, and three of them show a stronger up-regulation in *Fg*+OG10 compared to other treatments (TRITD7Av1G190220, Log2FC = 10.85; TRITD7Bv1G154140, Log2FC = 7.74; TRITD5Av1G158460, Log2FC = 8.29) (Supplementary Table S12). Alignment of their protein sequences highlights marked similarity (>45%) to AtCELLOX1 that is involved in oxidation, and consequent inactivation, of cellodextrins (CDs), a well-known class of cell-wall derived DAMPs (Souza et al., 2017). Furthermore, Locci et al. (2019) observed that the oxidized CDs are not a carbon source for the known pathogenic fungus *Botrytis cinerea* suggesting an indirect antimicrobial activity against pathogenic fungi. The "function" of the 5 BBE-1 family-related genes (as the expression average value of all the genes putatively belonging to BBE-l family), was not significantly different among *Fg*, *Fg*+OG10, and *Fg*+OG500 (ANOVA, $p > 0.05$; average expression values 3.49 ± 1.32, 6.25 ± 3.91, 3.57 ± 1.28, respectively); however, when only TRITD7Av1G190220, TRITD7Bv1G154140, and TRITD5Av1G158460 were considered, their average expression was significantly higher in *Fg*+OG10 (average of 8.96 ± 1.66) compared to that of *Fg* and *Fg*+OG500 (4.29 ± 0.92 and 4.39 ± 0.59, respectively; ANOVA, $p < 0.00001$).

Similar behavior was also detected for cytosolic serine/threonine-protein kinase (e.g. *PBS-LIKE*, *PBLs*) encoding genes and for the *ENHANCED DISEASE RESISTANCE4 (EDR4)* gene. In *Arabidopsis thaliana* PBLs are important transducers of danger signaling (Rao et al., 2018) while EDR4 modulates plant immunity by associating with clathrin and regulating the relocation of EDR1 (Wu et al., 2015) or by regulating the association of key signaling elements to inhibit cell death (Neubauer et al., 2020). We found both *PBL* and *EDR1* encoding paralogues to be up-regulated in all the infected samples, except *Fg*+CHIT100. Interestingly, *EDR1* was also up-regulated only in OG500 samples among those treated with

elicitors of immunity. Another interesting hint regards the expression of the regulatory protein *NPR1*, involved in the salicylic acid signaling pathway (Janda et al., 2015), found to be significantly overexpressed only in *Fg*+OG10 (Log2FC = 7.38), whereas, at the analyzed hpi, the Log2FC values for *Fg* and *Fg*+OG500 samples were 1.37 and 1.70, respectively.

As previously reported in Kazan & Gardiner (2018), several genes involved in plant cell wall synthesis and degradation were found to be regulated after *Fg* infection. Most of them were up-regulated in all the *Fg* infected plants (*Fg*, *Fg*+OG10, *Fg*+OG500; Supplementary Table S12). Among them, genes coding for pectin-modifying enzymes such as a *pectinesterase* (TRITD1Bv1G117660) and three putative *pectinesterase/pectinesterase inhibitors* (TRITD1Av1G166830, TRITD5Bv1G222340, TRITD1Bv1G152660), involved in plant resistance to necrotrophs by regulating the PME activity (Lionetti et al., 2017), resulted to be commonly up-regulated between the three diverse co-treatments. It is worth noting that the two last (TRITD5Bv1G222340 and TRITD1Bv1G152660) presented slightly higher Log2FC values in *Fg*+OG treatments with respect the *Fg* treatment. Moreover, a gene coding for a probable *pectinesterase* (TRITD2Av1G026410) and two genes coding for *pectinesterase inhibitors* (TRITD2Av1G261160, TRITD1Bv1G228800) were significantly up-regulated only in seedlings treated with OG10, whereas *Fg*+OG500 treated plants specifically displayed a higher expression of an *endo-1,4-beta-xylanase* (TRITD5Av1G136370) and an *alpha-1,3-arabinosyltransferase* (TRITD6Av1G190480). The expression of six *endoglucanases*, enzymes with a role in cell wall remodeling during pathogen infection, was found to be significantly up-regulated: two genes (TRITD1Av1G025050 and TRITD6Av1G192020) were expressed in *Fg*, *Fg*+OG10 and *Fg*+OG500 treated seedlings, while four genes were significantly up-regulated only in *Fg*+OG10. Several genes putatively involved in phenylpropanoid/lignin biosynthesis have been also identified as up-regulated after *Fg* infection (Supplementary Table S12). A different regulation in the two OG treatments has been revealed considering the coumarate *CoA ligase* genes: seven genes were differently regulated and, worth noting, this "function" (as the expression average value of all the gens belonging to this category) was differently up-regulated in the three conditions (0.33 in *Fg*, 2.80 in *Fg*+OG10 and 0.29 in *Fg*+OG500). A gene coding for a putative glycerol-3-phosphate acyltransferase *RAM2* (TRITD4Av1G006510), reported to provide precursors for the synthesis of secreted lipids such as cutin, was down-regulated in plants infected by the pathogen, while it resulted as not regulated in OG treated plants. It has been demonstrated that RAM2 proteins are required for the establishment of a functional root symbiosis, as the corresponding loss-of-function mutants are impaired in the formation of fully developed arbuscules (Luginbuehl and Oldroyd, 2017). Genes coding for four epoxide hydrolases, which could be involved in the biosynthesis of polyhydroxylated cutin monomers, resulted to be regulated in infected and OG cotreated plants, with differences in the expression correlated

with the OG dose (Supplementary Table S12). Particularly, TRITD6Av1G005800 presented a Log2FC value of 6.12 in *Fg*+OG500 *versus* a Log2FC value of 1.37 in *Fg*+OG10. Genes coding for 3-ketoacyl-CoA synthases, reported as a negative regulator in cuticular wax production (Huang et al., 2023), appeared to be significantly finely tuned in all the infected plants (Supplementary Table S12).

Changes in *F. graminearum* transcriptome mediated by OGs

For each inoculated sample, an average of 14% of not aligned reads to plant transcriptome were successfully aligned to available *Fg* transcriptome and ranged from 890,614 to 2,380,036 with an average of 1,527,554 (Supplementary Table S18). A very low percentage of reads aligned against fungal transcriptome for samples coming from infected plants treated with CHIT100 (approximately 0.02%; Supplementary Table S18). Total fungal read counts are reported in Supplementary Table S19. Identification of DEGs in *Fg* infecting durum wheat tissues upon treatment with OG500 revealed alterations in gene regulation, with a total of 61 genes showing differential expression compared to *Fg* in plants without cotreatment (38 up- and 23 down-regulated; Supplementary Table S20). On the other hand, only 7 DEGs (3 up- and 4 down-regulated) were found in the fungus in the presence of OG10 (Supplementary Table S21). Four genes (FGSG_03061T0, FGSG_03915T0, FGSG_02477T0, and FGSG_10675T0) were detected as DEGs in both conditions, with a similar expression pattern. Two genes, i.e., encoding a putative NADH-dehydrogenase (ubiquinone) (FGSG_02477T0) and a uncharacterized protein (FGSG_10675T0), were up-regulated by the two OG treatments, while two genes (FGSG_03061T0 and FGSG_03915T0, putatively coding for a sorbitol dehydrogenase and a flavin-containing monooxygenase, respectively) were down-regulated. One of the key factors contributing to the virulence of *Fg* is the production of mycotoxins, such as DON, whose synthesis involves genes collectively known as the *Tri* genes (Jiang et al., 2016). In *Fg*, *Fg*+OG10, and *Fg*+OG500, reads aligned with 13 *Tri* genes, but when compared to *Fg*, no significant differences were detected (DEGs showed padj > 0.05) and, for this reason, they were not further considered (Supplementary Table S22).

DISCUSSION

The use of elicitors, able to stimulate the plant innate immune system, represents a novel and promising strategy in crop protection, as an alternative to conventional pesticides. OGs are potent elicitors of immunity when applied exogenously as they trigger a wide range of defense responses including accumulation of phytoalexins in soybean (Davis et al., 1986), deposition of callose, production of reactive oxygen species (ROS) (Galletti et al., 2008; Gravino et al., 2017) and nitric oxide (NO) (Rasul et al., 2012)

in Arabidopsis, accumulation of SA in strawberry (Osorio et al., 2008), activation of defense related genes (Denoux et al., 2008; Gravino et al., 2017). It is worth noting that a dose-dependency for some elicitors, including OG and Flg22, have been already reported in the induction of defense response pathway in Arabidopsis seedlings (Denoux et al. 2008). Nevertheless, a clear demonstration of the OG capability to activate defense-associated responses and resistance against *Fg* in wheat is so far lacking. Here, when exogenously applied, OGs could restrict FHB symptoms in a dose-dependent manner both locally and systemically, therefore indicating that they are sensed as danger signals in different durum wheat tissues, *i.e.*, spikes and cotyledons. A slowed disease progression, accompanied by lower amount of fungus, was detected in infected wheat spikes cotreated with OGs compared to the ears inoculated with the *Fg* alone. Consequently, elicitor treatments positively impacted the agronomic and yield parameters as well. This study shows that exogenous application of OGs reduces the yield losses associated with FHB infection by 51.34%. Moreover, spikes cotreated with *Fg* and OGs displayed higher values compared to ears treated with the fungus alone in terms of number of seeds per spike and spikelet, primary spike weight, seed weight per spike and weight of 1000 seeds. Furthermore, it was observed that OGs and chitosan limit the shriveling of *Fg*-infected durum wheat seeds. Wheat spikes and seeds in *Fg*+CHIT100 cotreatment did not show differences compared to untreated condition. Such lack of disease symptoms could be explained by the chitosan capability to inhibit fungal spore germination, mycelium growth and virulence (Luan et al., 2022; Francesconi et al., 2021). Interestingly, a similar, but lower, inhibitory direct effect on *Fg* growth was also detected by adding different amounts of OGs to the fungal growth medium, hinting that, locally, OGs may act not only as an elicitor of wheat immunity but also as a blocker of fungal growth. OGs and CHIT triggered resistance to *Fg* also in 3-day-old Svevo seedlings. Noteworthy, none of the OG doses considered in this study altered fresh weight, root length and first leaf length compared to untreated plants. Conversely, CHIT strongly inhibited all the biometric parameters, hinting that shared and distinctive responses are activated in response to the two oligosaccharins both locally and systemically.

To deeper understand the genetic bases of the observed durum wheat behavior in response to OGs and CHIT as well as the OG dose-dependency effect on wheat response both in presence and absence of *Fg*, RNAseq analyses were carried out, showing that OGs, as CHIT, act as elicitors of immune responses. Results showed that the transcriptome profiles of plants were differently remodeled not only depending on the basis of the applied elicitors but also depending on the applied concentrations. Additionally, results also revealed differences in fungal reads within the transcriptomic data. The infected plants without OG treatment exhibited an increase in fungal reads, suggesting a high presence of *Fg*-related genetic material, while plants infected and cotreated with OG500 and OG10 displayed a reduction in fungal reads. This suggests that the application of OGs effectively slowed the fungal infection, resulting in a decreased abundance of Fusarium-related genetic material, also confirmed by fungal DNA quantification through

qPCRs. In agreement with previous published data on wheat response to pathogens (Anguelova-Merhar et al., 2001; Tripathi et al., 2013; Zhang et al., 2019), DEGs related to several defense genes, including those encoding for chitinases and β-1,3-glucanases, were identified. It is worth noting that different genes encoding for chitinases were found to be up-regulated in OG10 inoculated plants, while only one gene coding for a basic endochitinase-like (TRITD7Av1G248080) was up-regulated in OG500 treated seedlings, confirming the activation of different mechanisms depending on the OG concentration. Several genes have been differentially regulated in OG10 treatment and OG500 treatment, suggesting that wheat cotyledons can sense and respond specifically to different amounts of OGs. The differences observed among the two OG treatments, either in absence or presence of the pathogen, are also reflected by the GO enrichment profiles.

Among the genes exclusively up-regulated in OG500 treatment, a putative *polyamine oxidase-like* was found. It has been suggested that the production of hydrogen peroxide (H2O2) deriving from polyamine oxidation might be correlated with cell wall reinforcement during pathogen invasion, besides cell wall maturation and lignification during plant development. The H2O2 originated from polyamine oxidation may be involved as signal molecules in mediating cell death, the hypersensitive response, expression of defense genes (Cona et al., 2006) and recently has been shown to be involved in systemic wound-triggered stomatal closure (Fraudentali et al., 2023). Further, both *EDR4* and *NHL* gene, involved in the activation of plant defense responses to biotic stresses (Maldonado et al., 2014; Chen et al., 2018), were found to be up-regulated in response to OG500, confirming the regulation of defense-related genes mediated by these elicitors, independently from the presence of the pathogen. Expression of genes involved in plant cell wall metabolism was also altered, including genes involved in the phenylpropanoid pathway. Among them are genes encoding for caffeoylshikimate esterase (CSE)-like, involved in lignin biosynthesis (Vanholme et al., 2013). A CSE has been recently reported to be involved in mediating the cucumber disease resistance to a fungal attack by promoting lignin biosynthesis (Yu et al. 2022). In our experiment, four genes were upregulated in *Fg* and *Fg*+OG500, while only two appeared to be upregulated in *Fg*+OG10 treatments. Also, expansins, involved in plant cell wall remodeling (Cosgrove, 2000), were specifically regulated by OGs, in the presence or absence of *Fg*, whereas, noteworthy, none was significantly regulated by CHIT. A similar expression pattern was observed for genes related with the OG sensing and homeostasis, *i.e.*, cell wall associated kinases and BBE-l. Particularly, five genes correlated to BBE-l were up-regulated by the two doses of OGs in presence of the fungus.

On the other hand, in *Fg*, upon OG500 treatment, the downregulation of fungal genes related to energy production and conversion, lipid transport and metabolism, replication, carbohydrate transport and metabolism and amino acid metabolism suggested potential changes in various fungal cellular processes. It

could be hypothesized that these changes may have implications for the fungal growth and interactions with the plant host. The upregulation of *NADH-dehydrogenase* in *Fg* in plants treated either with OG10 and OG500 may suggest a protective role against oxidative stress. Previous studies have provided evidence that alternative NADH dehydrogenases in filamentous fungi exhibit increased activity in the presence of oxidative stress (Bai et al., 2003; Voulgaris al., 2012).

Moreover, downregulation of a putative fungal flavin-containing monooxygenase was found in both conditions with OGs. Flavin-containing monooxygenases have a broad distribution across different organisms and play diverse roles in various biological processes, including detoxification (van Berkel et al., 2006). It could be hypothesized that downregulation of a flavin-containing monooxygenase genes can affect fungal detoxification mechanisms, resulting in a reduced detoxification capacity. The lack of significant differences in Trichothecene biosynthetic gene (*Tri*) gene expression between *Fg*-infected with OG and *Fg*-infected plants may be explained by the possibility that the time point at which the samples were collected might not have captured the dynamic changes in *Tri* gene expression (Lee et al., 2014). Additional time-course experiments with multiple sampling points would be beneficial in elucidating the temporal dynamics of *Tri* gene expression during *Fg* infection with and without OG application.

Overall, transcriptomics data showed that specific plant responses were observed in the diverse treatments (different elicitors and doses), also in the absence of the fungal pathogen. Results demonstrated that OGs, like chitosan, limit the spread of the *Fg* in durum wheat plant tissues and, possibly, decrease the mycotoxin contamination and shed light on the functionality of OGs as elicitors of immunity and their ability in protecting a cereal like durum wheat, characterized by a high susceptibility to FHB. Exogenous application of OGs led to a significant decrease of FHB lesion sizes and disease severity on wheat coleoptiles and spikes, respectively. This is the first observation of direct involvement of OGs in enhancing resistance against the *Fg* phytopathogen.

The improvement of natural plant defense mechanisms to control pathogen attacks is one of the most attracting strategies to increase resistance in a sustainable manner. In this scenario, the use of cell wall derived elicitors, such as OGs, able to stimulate the plant innate immune system, represents a novel and promising strategy in crop protection, as an alternative to conventional pesticides (Alexandersson et al., 2016; Iriti and Varoni, 2017). Based on the knowledge that OGs may activate a wide range of defense responses, it will be of interest, in the next future, to generate and analyze durum wheat lines with altered capability in producing and/or sensing OGs.

Author contributions

D.V.S. and R.B. designed the experiments. V.B. performed pathogenic bioassays and analyses in spikes. V.B. and S.G. performed pathogenic bioassays and analyses in seedlings. F.S. and L.G. performed transcriptomic analyses. D.P. prepared OGs. D.V.S. and R.B. prepared the article. V.B. and F.S. prepared the figures. All authors contributed to the article and approved the submitted version.

Funding statement

This study was carried out within the Agritech National Research Center and received funding from the European Union Next-Generation EU (PIANO NAZIONALE DI RIPRESA E RESILIENZA (PNRR) – MISSIONE 4 COMPONENTE 2, INVESTIMENTO 1.4 – D.D. 1032 17/06/2022, CN00000022). This manuscript reflects only the authors' views and opinions, neither the European Union nor the European Commission can be considered responsible for them. Transcriptomics and LG fellowship were funded by the PRIMA project OPTIMUS PRIME (MUR DD 16302, 12/11/2021).

Conflict of interest

Authors have no conflict of interest to declare.

Data availability

Data generated in this study are available in the Supplementary Information of this paper. RNA-seq reads were submitted to NCBI Sequence Read Archive (SRA) under BioProject accession number PRJNA977839.

References

Abdul Malik, N. A., Kumar, I. S., and Nadarajah, K. (2020). Elicitor and receptor molecules: Orchestrators of plant defense and immunity. *International Journal of Molecular Sciences*, **21**, 963.

Alexandersson, E., Mulugeta, T., Lankinen, Å., Liljeroth, E., and Andreasson, E. (2016). Plant resistance inducers against pathogens in Solanaceae species-from molecular mechanisms to field application. *International Journal of Molecular Sciences*, **17**, 1673.

Alisaac, E., and Mahlein, A. K. (2023). Fusarium head blight on wheat: Biology, modern detection and diagnosis and integrated disease management. *Toxins*, **15**, 192.

Anguelova- Merhar, V. S., VanDer Westhuizen, A. J., and Pretorius, Z. A. (2001). β- 1, 3- glucanase and chitinase activities and the resistance response of wheat to leaf rust. *Journal of Phytopathology*, **149**, 381-384.

Aziz, A., Trotel-Aziz, P., Dhuicq, L., Jeandet, P., Couderchet, M., and Vernet, G. (2006). Chitosan oligomers and copper sulfate induce grapevine defense reactions and resistance to gray mold and downy mildew. *Phytopathology*, **96**, 1188-1194.

Bai, Z., Harvey, L. M., and McNeil, B. (2003). Oxidative stress in submerged cultures of fungi. *Critical Reviews in Biotechnology*, **23**, 267-302.

Benedetti, M., Verrascina, I., Pontiggia, D., Locci, F., Mattei, B., De Lorenzo, G., and Cervone, F. (2018). Four Arabidopsis berberine bridge enzyme- like proteins are specific oxidases that inactivate the elicitor- active oligogalacturonides. *The Plant Journal*, **94**, 260-273.

Benedetti, M., Locci, F., Gramegna, G., Sestili, F., and Savatin, D. V. (2019). Green production and biotechnological applications of cell wall lytic enzymes. *Applied Sciences*, **9**, 5012.

Bhat, N.N., Padder, B.A., Barthelson, R.A., and Andrabi, K.I. (2019). Compendium of *Colletotrichum graminicola* responsive infection-induced transcriptomic shifts in the maize. *Plant Gene*, **17**, 100166.

Bian, C., Duan, Y., Xiu, Q., Wang, J., Tao, X., and Zhou, M. (2021). Mechanism of validamycin A inhibiting DON biosynthesis and synergizing with DMI fungicides against *Fusarium graminearum*. *Molecular Plant Pathology*, **22**, 769-785.

Bigini, V., Camerlengo, F., Botticella, E., Sestili, F., and Savatin, D. V. (2021). Biotechnological resources to increase disease-resistance by improving plant immunity: A sustainable approach to save cereal crop production. *Plants*, **10**, 1146.

Boedi, S., Berger, H., Sieber, C., Münsterkötter, M., Maloku, I., Warth, B., and Strauss, J. (2016). Comparison of *Fusarium graminearum* transcriptomes on living or dead wheat differentiates substrate-responsive and defense-responsive genes. *Frontiers in Microbiology*, **7**, 1113.

Botticella, E., Savatin, D. V., and Sestili, F. (2021). The triple jags of dietary fibers in cereals: How biotechnology is longing for high fiber grains. *Frontiers in Plant Science*, **12**, 745579.

Brown, N. A., Urban, M., Van de Meene, A. M., and Hammond-Kosack, K. E. (2010). The infection biology of *Fusarium graminearum*: defining the pathways of spikelet to spikelet colonisation in wheat ears. *Fungal Biology*, **114**, 555-571.

Chanda, B., Xia, Y. E., Mandal, M. K., Yu, K., Sekine, K. T., Gao, Q. M., and Kachroo, P. (2011). Glycerol-3-phosphate is a critical mobile inducer of systemic immunity in plants. *Nature Genetics*, **43**, 421-427.

Chang, S., Puryear, J., and Cairney, J. (1993). A simple and efficient method for isolating RNA from pine trees. *Plant Molecular Biology Reporter*, **11**, 113-116.

Chen, L., Wang, H., Yang, J., Yang, X., Zhang, M., Zhao, Z., and Wang, J. (2021). Bioinformatics and transcriptome analysis of CFEM proteins in *Fusarium graminearum*. *Journal of Fungi*, **7**, 871.

Chen, Q., Tian, Z., Jiang, R., Zheng, X., Xie, C., and Liu, J. (2018). StPOTHR1, a NDR1/HIN1-like gene in *Solanum tuberosum*, enhances resistance against *Phytophthora infestans*. *Biochemical and Biophysical Research Communications*, **496**, 1155-1161.

Cona, A., Rea, G., Angelini, R., Federico, R., and Tavladoraki, P. (2006). Functions of amine oxidases in plant development and defence. *Trends in Plant Science*, **11**, 80-88.

Conesa, A., Götz, S., García-Gómez, J. M., Terol, J., Talón, M., and Robles, M. (2005). Blast2GO: a universal tool for annotation, visualization and analysis in functional genomics research. *Bioinformatics*, **21**(18), 3674-3676.

Cosgrove, D. (2000). Loosening of plant cell walls by expansins. *Nature*, **407**, 321–326.

Cuomo, C. A., Güldener, U., Xu, J. R., Trail, F., Turgeon, B. G., Di Pietro, A., and Kistler, H. C. (2007). The *Fusarium graminearum* genome reveals a link between localized polymorphism and pathogen specialization. *Science*, **317**, 1400-1402.

Davidsson, P., Broberg, M., Kariola, T., Sipari, N., Pirhonen, M., and Palva, E. T. (2017). Short oligogalacturonides induce pathogen resistance-associated gene expression in *Arabidopsis thaliana*. *BMC Plant Biology*, **17**, 1-17.

Davis, K. R., Darvill, A. G., Albersheim, P., and Dell, A. (1986). Host-pathogen interactions: XXIX. Oligogalacturonides released from sodium polypectate by endopolygalacturonic acid lyase are elicitors of phytoalexins in soybean. *Plant Physiology*, **80**, 568-577.

De Lorenzo, G., and Cervone, F. (2022). Plant immunity by damage-associated molecular patterns (DAMPs). *Essays in Biochemistry*, **66**, 459-469.

Denoux, C., Galletti, R., Mammarella, N., Gopalan, S., Werck, D., De Lorenzo, G., and Dewdney, J. (2008). Activation of defense response pathways by OGs and Flg22 elicitors in Arabidopsis seedlings. *Molecular Plant*, **1**, 423-445.

Desaki, Y., Otomo, I., Kobayashi, D., Jikumaru, Y., Kamiya, Y., Venkatesh, B., and Shibuya, N. (2012). Positive crosstalk of MAMP signaling pathways in rice cells. *PLoS One*, **7**, e51953.

Deshaies, M., Lamari, N., Ng, C. K., Ward, P., and Doohan, F. M. (2022). The impact of chitosan on the early metabolomic response of wheat to infection by *Fusarium graminearum*. *BMC Plant Biology*, **22**, 73.

Ding, L., Xu, H., Yi, H., Yang, L., Kong, Z., Zhang, L., and Ma, Z. (2011). Resistance to hemi-biotrophic *F. graminearum* infection is associated with coordinated and ordered expression of diverse defense signaling pathways. *PloS one*, **6**, e19008.

Erayman, M., Turktas, M., Akdogan, G., Gurkok, T., Inal, B., Ishakoglu, E., and Unver, T. (2015). Transcriptome analysis of wheat inoculated with *Fusarium graminearum*. *Frontiers in Plant Science*, **6**, 867.

Ferrari, S., Galletti, R., Denoux, C., De Lorenzo, G., Ausubel, F. M., and Dewdney, J. (2007). Resistance to *Botrytis cinerea* induced in Arabidopsis by elicitors is independent of salicylic acid, ethylene, or jasmonate signaling but requires PHYTOALEXIN DEFICIENT3. *Plant Physiology*, **144**, 367-379.

Ferrari, S., Savatin, D. V., Sicilia, F., Gramegna, G., Cervone, F., and Lorenzo, G. D. (2013). Oligogalacturonides: plant damage-associated molecular patterns and regulators of growth and development. *Frontiers in Plant Science*, **4**, 49.

Francesconi, S., Steiner, B., Buerstmayr, H., Lemmens, M., Sulyok, M., and Balestra, G. M. (2020). Chitosan hydrochloride decreases *Fusarium graminearum* growth and virulence and boosts growth, development and systemic acquired resistance in two durum wheat genotypes. *Molecules*, **25**, 4752.

Fraudentali, I., Pedalino, C., D'Incà, R., Tavladoraki, P., Angelini, R., and Cona, A. (2023). Distinct role of AtCuAOβ-and RBOHD-driven H2O2 production in wound-induced local and systemic leaf-to-leaf and root-to-leaf stomatal closure. *Frontiers in Plant Science*, **14**, 1154431.

Galletti, R., Denoux, C., Gambetta, S., Dewdney, J., Ausubel, F. M., De Lorenzo, G., and Ferrari, S. (2008). The AtrbohD-mediated oxidative burst elicited by oligogalacturonides in Arabidopsis is dispensable for the activation of defense responses effective against *Botrytis cinerea*. *Plant Physiology*, **148**, 1695-1706.

Gamir, J., Minchev, Z., Berrio, E., García, J. M., De Lorenzo, G., & Pozo, M. J. (2021). Roots drive oligogalacturonide- induced systemic immunity in tomato. *Plant, Cell & Environment*, **44**, 275-289.

Ge, S. X., Jung, D., and Yao, R. (2020). ShinyGO: a graphical gene-set enrichment tool for animals and plants. *Bioinformatics*, **36**, 2628-2629.

Gravino, M., Locci, F., Tundo, S., Cervone, F., Savatin, D. V., and De Lorenzo, G. (2017). Immune responses induced by oligogalacturonides are differentially affected by AvrPto and loss of BAK1/BKK1 and PEPR1/PEPR2. *Molecular Plant Pathology*, **18**, 582-595.

Häggblom, P., and Nordkvist, E. (2015). Deoxynivalenol, zearalenone, and *Fusarium graminearum* contamination of cereal straw; field distribution; and sampling of big bales. *Mycotoxin research*, **31**, 101-107.

Hahn, M. G., Darvill, A. G., and Albersheim, P. (1981). Host-pathogen interactions: XIX. The endogenous elicitor, a fragment of a plant cell wall polysaccharide that elicits phytoalexin accumulation in soybeans. *Plant Physiology*, **68**, 1161-1169.

Henrissat, B. (1991). A classification of glycosyl hydrolases based on amino acid sequence similarities. *Biochemical Journal*, **280**, 309-316.

Huang, H., Yang, X., Zheng, M., Chen, Z., Yang, Z., Wu, P., and Zhao, H. (2023). An ancestral role for 3-KETOACYL-COA SYNTHASE3 as a negative regulator of plant cuticular wax synthesis. *The Plant Cell*, **35**, 2251-2270.

Iriti, M., and Varoni, E. M. (2017). Moving to the field: Plant innate immunity in crop protection. *International Journal of Molecular Sciences*, **18**, 640.

Janda, M., and Ruelland, E. (2015). Magical mystery tour: Salicylic acid signalling. *Environmental and Experimental Botany*, **114**, 117-128.

Jansen, C., Von Wettstein, D., Schäfer, W., Kogel, K. H., Felk, A., and Maier, F. J. (2005). Infection patterns in barley and wheat spikes inoculated with wild-type and trichodiene synthase gene disrupted *Fusarium graminearum*. *Proceedings of the National Academy of Sciences*, **102**, 16892-16897.

Jia, L. J., Wang, W. Q., and Tang, W. H. (2017). Wheat coleoptile inoculation by *Fusarium graminearum* for large-scale phenotypic analysis. *Bio-Protocol*, **7**, e2439-e2439.

Jiang, C., Zhang, C., Wu, C., Sun, P., Hou, R., Liu, H., Wang, C., and Xu, J. R. (2016). *TRI6* and *TRI10* play different roles in the regulation of deoxynivalenol (DON) production by cAMP signalling in *Fusarium graminearum*. *Environmental Microbiology*, **18**, 3689-3701.

Jung, J. Y., Kim, J. H., Baek, M., Cho, C., Cho, J., Kim, J., and Kim, K. H. (2022). Adapting to the projected epidemics of Fusarium head blight of wheat in Korea under climate change scenarios. *Frontiers in Plant Science*, **13**.

Kazan, K., and Gardiner, D. M. (2018). Fusarium crown rot caused by *Fusarium pseudograminearum* in cereal crops: recent progress and future prospects. *Molecular Plant Pathology*, **19**(7), 1547-1562.

Kubicek, C. P., Starr, T. L., and Glass, N. L. (2014). Plant cell wall–degrading enzymes and their secretion in plant-pathogenic fungi. *Annual Review of Phytopathology*, **52**, 427-451.

Lee, T., Lee, S. H., Shin, J. Y., Kim, H. K., Yun, S. H., Kim, H. Y., and Ryu, J. G. (2014). Comparison of trichothecene biosynthetic gene expression between *Fusarium graminearum* and *Fusarium asiaticum*. *The Plant Pathology Journal*, **30**, 33.

Lionetti, V., Fabri, E., De Caroli, M., Hansen, A. R., Willats, W. G., Piro, G., and Bellincampi, D. (2017). Three pectin methylesterase inhibitors protect cell wall integrity for Arabidopsis immunity to *Botrytis*. *Plant Physiology*, **173**, 1844-1863.

Liu, R. Q., Li, J. C., Wang, Y. S., Zhang, F. L., Li, D. D., Ma, F. X., and Chen, X. L. (2021). Amino-oligosaccharide promote the growth of wheat, increased antioxidant enzymes activity. *Biology Bulletin*, **48**, 459-467.

Livak, K. J., and Schmittgen, T. D. (2001). Analysis of relative gene expression data using real-time quantitative PCR and the $2^{-\Delta\Delta CT}$ method. *Methods*, **25**, 402–408.

Locci, F., Benedetti, M., Pontiggia, D., Citterico, M., Caprari, C., Mattei, B., and De Lorenzo, G. (2019). An Arabidopsis berberine bridge enzyme- like protein specifically oxidizes cellulose oligomers and plays a role in immunity. *The Plant Journal*, **98**, 540-554.

Love, M. I., Huber, W., and Anders, S. (2014). Moderated estimation of fold change and dispersion for RNA-seq data with DESeq2. *Genome Biology*, **15**, 1-21.

Luan, J., Wei, X., Li, Z., Tang, W., Yang, F., Yu, Z., and Li, X. (2022). Inhibition of Chitosan with Different Molecular Weights on Barley-Borne *Fusarium graminearum* during Barley Malting Process for Improving Malt Quality. *Foods*, **11**, 3058.

Luginbuehl, L. H., and Oldroyd, G. E. (2017). Understanding the arbuscule at the heart of endomycorrhizal symbioses in plants. *Current Biology*, **27**, R952-R963.

Maccaferri, M., Harris, N. S., Twardziok, S. O., Pasam, R. K., Gundlach, H., Spannagl, M., and Cattivelli, L. (2019). Durum wheat genome highlights past domestication signatures and future improvement targets. *Nature Genetics*, **51**, 885-895.

Magan, N., and Aldred, D. (2007). Post-harvest control strategies: minimizing mycotoxins in the food chain. *International Journal of Food Microbiology*, **119**, 131-139.

Makandar, R., Nalam, V. J., Lee, H., Trick, H. N., Dong, Y., and Shah, J. (2012). Salicylic acid regulates basal resistance to Fusarium head blight in wheat. *Molecular Plant-Microbe Interactions*, **25**(3), 431-439.

Maldonado, A., Youssef, R., McDonald, M., Brewer, E., Beard, H., and Matthews, B. (2014). Overexpression of four *Arabidopsis thaliana* NHL genes in soybean (*Glycine max*) roots and their effect on resistance to the soybean cyst nematode (*Heterodera glycines*). *Physiological and Molecular Plant Pathology*, **86**, 1-10.

Mary Wanjiru, W., Zhensheng, K., and Buchenauer, H. (2002). Importance of cell wall degrading enzymes produced by *Fusarium graminearum* during infection of wheat heads. *European Journal of Plant Pathology*, **108**, 803-810.

Miedaner, T. (1997). Breeding wheat and rye for resistance to Fusarium diseases. *Plant Breeding*, **116**, 201-220.

Miedaner, T., Sieber, A. N., Desaint, H., Buerstmayr, H., Longin, C. F. H., and Würschum, T. (2017). The potential of genomic- assisted breeding to improve Fusarium head blight resistance in winter durum wheat. *Plant Breeding*, **136**, 610-619.

Miranda, J. H., Williams, R. W., and Kerven, G. (2007). Galacturonic acid-induced changes in strawberry plant development in vitro. *In Vitro Cellular & Developmental Biology-Plant*, **43**, 639-643.

Montesano, M., Kõiv, V., Mäe, A., and Palva, E. T. (2001). Novel receptor- like protein kinases induced by *Erwinia carotovora* and short oligogalacturonides in potato. *Molecular Plant Pathology*, **2**, 339-346.

Moscatiello, R., Mariani, P., Sanders, D., and Maathuis, F. J. (2006). Transcriptional analysis of calcium-dependent and calcium-independent signalling pathways induced by oligogalacturonides. *Journal of Experimental Botany*, **57**, 2847-2865.

Neubauer, M., Serrano, I., Rodibaugh, N., Bhandari, D. D., Bautor, J., Parker, J. E., and Innes, R. W. (2020). Arabidopsis EDR1 protein kinase regulates the association of EDS1 and PAD4 to inhibit cell death. *Molecular Plant-Microbe Interactions*, **33**, 693-703.

Norman, C., Vidal, S., and Palva, E. T. (1999). Oligogalacturonide-mediated induction of a gene involved in jasmonic acid synthesis in response to the cell-wall-degrading enzymes of the plant pathogen *Erwinia carotovora*. *Molecular Plant-Microbe Interactions*, **12**, 640-644.

Nothnagel, E. A., McNeil, M., Albersheim, P., and Dell, A. (1983). Host-pathogen interactions: XXII. A galacturonic acid oligosaccharide from plant cell walls elicits phytoalexins. *Plant Physiology*, **71**, 916-926.

Ochoa-Meza, L. C., Quintana-Obregón, E. A., Vargas-Arispuro, I., Falcón-Rodríguez, A. B., Aispuro-Hernández, E., Virgen-Ortiz, J. J., and Martínez-Téllez, M. Á. (2021). Oligosaccharins as elicitors of defense responses in wheat. *Polymers*, **13**, 3105.

Osorio, S., Castillejo, C., Quesada, M. A., Medina- Escobar, N., Brownsey, G. J., Suau, R., and Valpuesta, V. (2008). Partial demethylation of oligogalacturonides by pectin methyl esterase 1 is required for eliciting defence responses in wild strawberry (*Fragaria vesca*). *The Plant Journal*, **54**, 43-55.

Patro, R., Duggal, G., Love, M. I., Irizarry, R. A., and Kingsford, C. (2017). Salmon provides fast and bias-aware quantification of transcript expression. *Nature Methods*, **14**, 417-419.

Pfaffl, M. W. (2001). A new mathematical model for relative quantification in real-time RT–PCR. *Nucleic Acids Research*, **29**, e45-e45.

Pontiggia, D., Ciarcianelli, J., Salvi, G., Cervone, F., De Lorenzo, G., and Mattei, B. (2015). Sensitive detection and measurement of oligogalacturonides in Arabidopsis. *Frontiers in Plant Science*, **6**, 258.

Pontiggia, D., Benedetti, M., Costantini, S., De Lorenzo, G., and Cervone, F. (2020). Dampening the DAMPs: How plants maintain the homeostasis of cell wall molecular patterns and avoid hyper-immunity. *Frontiers in Plant Science*, **11**, 613259.

Randoux, B., Renard-Merlier, D., Mulard, G., Rossard, S., Duyme, F., Sanssené, J., and Reignault, P. (2010). Distinct defenses induced in wheat against powdery mildew by acetylated and nonacetylated oligogalacturonides. *Phytopathology*, **100**, 1352-1363.

Rao, S., Zhou, Z., Miao, P., Bi, G., Hu, M., Wu, Y., and Zhou, J. M. (2018). Roles of receptor-like cytoplasmic kinase VII members in pattern-triggered immune signaling. *Plant Physiology*, **177**, 1679-1690.

Rasul, S., Dubreuil- Maurizi, C., Lamotte, O., Koen, E., Poinssot, B., Alcaraz, G., and Jeandroz, S. (2012). Nitric oxide production mediates oligogalacturonide- triggered immunity and resistance to *Botrytis cinerea* in *Arabidopsis thaliana*. *Plant, Cell & Environment*, **35**, 1483-1499.

Savary, S., Willocquet, L., Pethybridge, S. J., Esker, P., McRoberts, N., and Nelson, A. (2019). The global burden of pathogens and pests on major food crops. *Nature Ecology & Evolution*, **3**, 430-439.

Savatin, D. V., Gramegna, G., Modesti, V., and Cervone, F. (2014). Wounding in the plant tissue: the defense of a dangerous passage. *Frontiers in Plant Science*, **5**, 470.

Simpson, S. D., Ashford, D. A., Harvey, D. J., and Bowles, D. J. (1998). Short chain oligogalacturonides induce ethylene production and expression of the gene encoding aminocyclopropane 1-carboxylic acid oxidase in tomato plants. *Glycobiology*, **8**, 579-583.

Soneson, C., Love, M. I., and Robinson, M. D. (2015). Differential analyses for RNA-seq: transcript-level estimates improve gene-level inferences. *F1000Research*, **4**.

Sorrentino, M., De Diego, N., Ugena, L., Spíchal, L., Lucini, L., Miras-Moreno, B., Zhang, L., Rouphael, Y., Colla, G., and Panzarová, K. (2021) Seed priming with protein hydrolysates improves Arabidopsis growth and stress tolerance to abiotic stresses. *Frontiers in Plant Science*, **12**, 626301.

Souza, C. A., Li, S., Lin, A. Z., Boutrot, F., Grossmann, G., Zipfel, C., and Somerville, S. C. (2017). Cellulose-derived oligomers act as damage-associated molecular patterns and trigger defense-like responses. *Plant Physiology*, **173**, 2383–2398.

Steiner, B., Buerstmayr, M., Michel, S., Schweiger, W., Lemmens, M., and Buerstmayr, H. (2017). Breeding strategies and advances in line selection for Fusarium head blight resistance in wheat. *Tropical Plant Pathology*, **42**, 165-174.

Steiner, B., Michel, S., Maccaferri, M., Lemmens, M., Tuberosa, R., and Buerstmayr, H. (2019). Exploring and exploiting the genetic variation of Fusarium head blight resistance for genomic-assisted breeding in the elite durum wheat gene pool. *Theoretical and Applied Genetics*, **132**, 969-988.

Trail, F. (2009). For blighted waves of grain: *Fusarium graminearum* in the postgenomics era. *Plant Physiology*, **149**, 103-110.

Tripathi, A., Aggarwal, R., and Yadav, A. (2013). Differential expression analysis of defense-related genes responsive to *Tilletia indica* infection in wheat. *Turkish Journal of Biology*, **37**, 606-613.

Urban, M., Daniels, S., Mott, E., and Hammond- Kosack, K. (2002). Arabidopsis is susceptible to the cereal ear blight fungal pathogens *Fusarium graminearum* and *Fusarium culmorum*. *The Plant Journal*, **32**, 961-973.

Van Berkel, W. J. H., Kamerbeek, N. M., and Fraaije, M. (2006). Flavoprotein monooxygenases, a diverse class of oxidative biocatalysts. *Journal of Biotechnology*, **124**, 670-689.

Vanholme, R., Cesarino, I., Rataj, K., Xiao, Y., Sundin, L., Goeminne, G., and Boerjan, W. (2013). Caffeoyl shikimate esterase (CSE) is an enzyme in the lignin biosynthetic pathway in Arabidopsis. *Science*, **341**, 1103-1106.

Voulgaris, I., O'Donnell, A., Harvey, L. M., and McNeil, B. (2012). Inactivating alternative NADH dehydrogenases: enhancing fungal bioprocesses by improving growth and biomass yield?. *Scientific Reports*, **2**, 1-9.

Yang, F. E. N., Jensen, J. D., Svensson, B., Jørgensen, H. J., Collinge, D. B., and Finnie, C. (2012). Secretomics identifies *Fusarium graminearum* proteins involved in the interaction with barley and wheat. *Molecular Plant Pathology*, **13**, 445-453.

Wan, J., He, M., Hou, Q., Zou, L., Yang, Y., Wei, Y., and Chen, X. (2021). Cell wall associated immunity in plants. *Stress Biology*, **1**, 3.

Wu, G., Liu, S., Zhao, Y., Wang, W., Kong, Z., and Tang, D. (2015). ENHANCED DISEASE RESISTANCE4 associates with CLATHRIN HEAVY CHAIN2 and modulates plant immunity by regulating relocation of EDR1 in Arabidopsis. *The Plant Cell*, **27**, 857-873.

Zhang, S. B., Zhang, W. J., Zhai, H. C., Lv, Y. Y., Cai, J. P., Jia, F., and Hu, Y. S. (2019). Expression of a wheat β-1, 3-glucanase in *Pichia pastoris* and its inhibitory effect on fungi commonly associated with wheat kernel. *Protein Expression and Purification*, **154**, 134-139.

Zhang, X. W., Jia, L. J., Zhang, Y., Jiang, G., Li, X., Zhang, D., and Tang, W. H. (2012). In planta stage-specific fungal gene profiling elucidates the molecular strategies of *Fusarium graminearum* growing inside wheat coleoptiles. *The Plant Cell*, **24**, 5159-5176.

Legends

Figure 1. OGs trigger resistance to FHB in *cv*. Svevo spikes. **A)** Disease severity in the cultivar Svevo inoculated with *Fg* and *Fg*+OG or *Fg*+CHIT cotreatment. Disease progression was monitored for 21 dpi; **B)** *Fg* DNA quantification by real-time PCR analysis of *β-tubulin* gene normalized to the *TdACTIN* gene in spikes at 6, 24, 48 hpi.; **C)** Images showing disease spread in representative wheat spikes for each treatment condition. Images were taken at 10 dpi. All values are the means ± SE (n = 15). Asterisks above the bars indicate values that are significantly different from seedlings inoculated with the *Fg* alone (*** $p < 0.01$, student t-test).

Figure 2. Agronomic and growth parameters in OG- and CHIT-cotreated wheat plants after *F. graminearum* infection. A) Number of seeds per spike; **B)** Number of seeds per spikelet; **C)** Primary spike weight (g); **D)** Seed weight per spike (g); **E)** Weight 1000 seeds (g); **F)** Yield loss (%) for the wheat *cv*. Svevo. A minimum of 10 plants per treatment condition were analyzed to obtain data. All values are the means ± standard error (SE). The statistical significance was tested by means of ANOVA followed by Tukey test. Different letters indicate statistically different values ($p < 0.05$).

Figure 3. Seed quality and filling in OG- and CHIT-cotreated wheat plants after *F. graminearum* infection. A) Seed length (mm); **B)** Seed width (mm); **C)** Pictures showing length and width of representative seeds for each treatment condition. Ten seeds per treatment were analyzed to obtain data. All values are the means ± standard error (SE). The statistical significance was tested by means of ANOVA followed by Tukey test. Different letters indicate statistically different values ($p < 0.05$).

Figure 4. Effects on morphological parameters of wheat seedlings grown in MS medium in the absence or presence of different concentrations of purified OGs or CHIT. A) Fresh weight; **B)** Root length; **C)** First leaf length. The measurements were carried out 7 days after transplanting in MS medium. The statistical significance was tested by means of ANOVA followed by Tukey test. Different letters indicate statistically different values ($p < 0.05$).

Figure 5. OGs trigger local and systemic resistance to FHB in a dose-dependent manner. Coleoptile lesion size in Svevo seedlings locally co- treated with *Fg*, *Fg*+OGs or *Fg*+CHIT (**A**) or grown in the absence or presence of the indicated amounts of elicitors for 3 days and then inoculated with *Fg* spores (**D**). Disease symptoms were monitored for 7 days post inoculation (dpi). **B** and **E**) Fungal genomic DNA quantification by real-time PCR analyses of the *Fgβ-tubulin* gene normalized to the wheat *TdACTIN* gene in wheat coleoptiles at 7 dpi; **C** and **F**) Images taken at 7 dpi showing disease spread in representative wheat coleoptiles for each treatment condition. All values are the means ± SE (n = 10). Asterisks above the bars indicate values that are significantly different from seedlings inoculated with the *Fg* alone (* $p < 0.05$, ** $p < 0.03$, *** $p < 0.01$, student t-test).

Figure 6. Heatmap and Venn diagrams depicting DEGs in the conditions *Fg*, *Fg*+OG10, *Fg*+OG500, *Fg*+CHIT100 *vs* control condition (mock). In (**A**), heatmap and hierarchical clustering of DEGs using the McQuitty algorithm. The heatmap shows the expression patterns of DEGs across four conditions compared to control one (mock), with red levels indicating up-regulated and green representing down-regulated DEGs. Different color intensity indicates different levels of expression (Log2Fold Change). In (**B**) and (**C**), Venn diagrams illustrate the overlap of up- and downregulated DEGs, respectively, between pairwise comparisons of the treatments.

Figure 7. **Heatmap depicting expression of 59 up-regulated DEGs shared by condition *Fg*, *Fg*+OG500 and OG500.** These shared DEGs may be related to a common response mediated by *Fg* and OG 500 µg/ml. Different color intensity indicates different levels of expression (Log2Fold Change).

Figure 8. Bubble plots showing GO-enriched terms classified as Biological Process (BP) in detected DEGs. In detail, enriched terms in OG10 (**A**), OG500 (**B**), and CHIT100 (**C**) are reported. The x-axis shows the fold enrichment values, *i.e.*, the percentage of genes in the selected DEG list belonging to a pathway divided by the corresponding percentage in the all reference gene list, and the y-axis reports the GO terms. Sizes of bubbles are proportional to the number of genes assigned to the related GO term, while bubbles color indicates the significance of the enriched term (False Discovery Rate values) as calculated by the enrichment analysis by Blast2GO.

Figure 9. Bubble plots showing GO-enriched terms classified as Biological Process (BP) in detected DEGs. In detail, enriched terms in *Fg* (**A**), *Fg*+OG10 (**B**), *Fg*+OG500 (**C**), and *Fg*+CHIT100 (**D**), are reported. The x-axis shows the fold enrichment values, i.e. the percentage of genes in the selected DEG list belonging to a pathway divided by the corresponding percentage in the all reference gene list, and the y-axis reports the GO terms. Sizes of bubbles are proportional to the number of genes assigned to the related GO term, while bubbles color indicates the significance of the enriched term (False Discovery Rate values) as calculated by the enrichment analysis by Blast2GO.

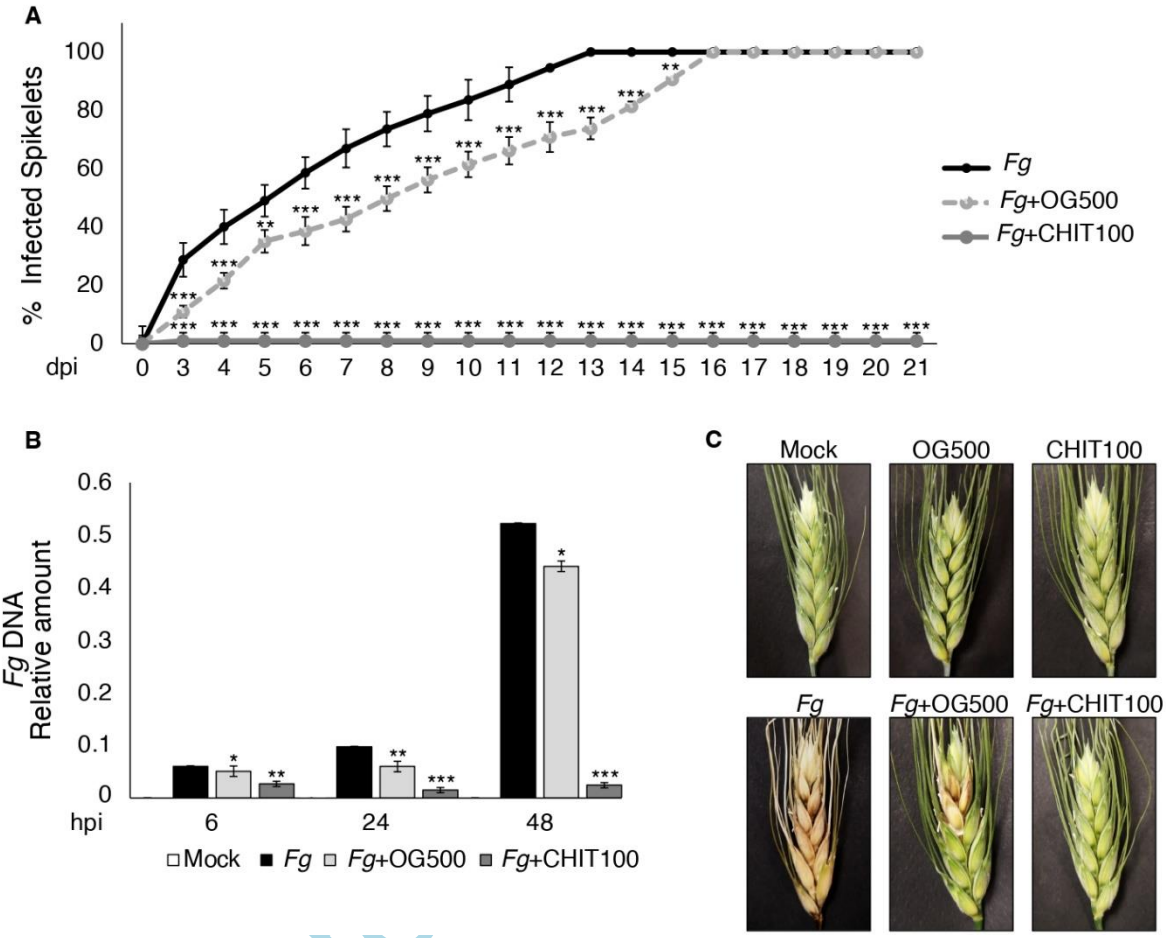

Figure 1. OGs trigger resistance to FHB in cv. Svevo spikes. **A)** Disease severity in the cultivar Svevo inoculated with *Fg* and *Fg*+OG or *Fg*+CHIT cotreatment. Disease progression was monitored for 21 dpi; **B)** *Fg* DNA quantification by real-time PCR analysis of *β-tubulin* gene normalized to the *TdACTIN* gene in spikes at 6, 24, 48 hpi.; **C)** Images showing disease spread in representative wheat spikes for each treatment condition. Images were taken at 10 dpi. All values are the means ± SE (n = 15). Asterisks above the bars indicate values that are significantly different from seedlings inoculated with the *Fg* alone (*** $p < 0.01$, student t-test).

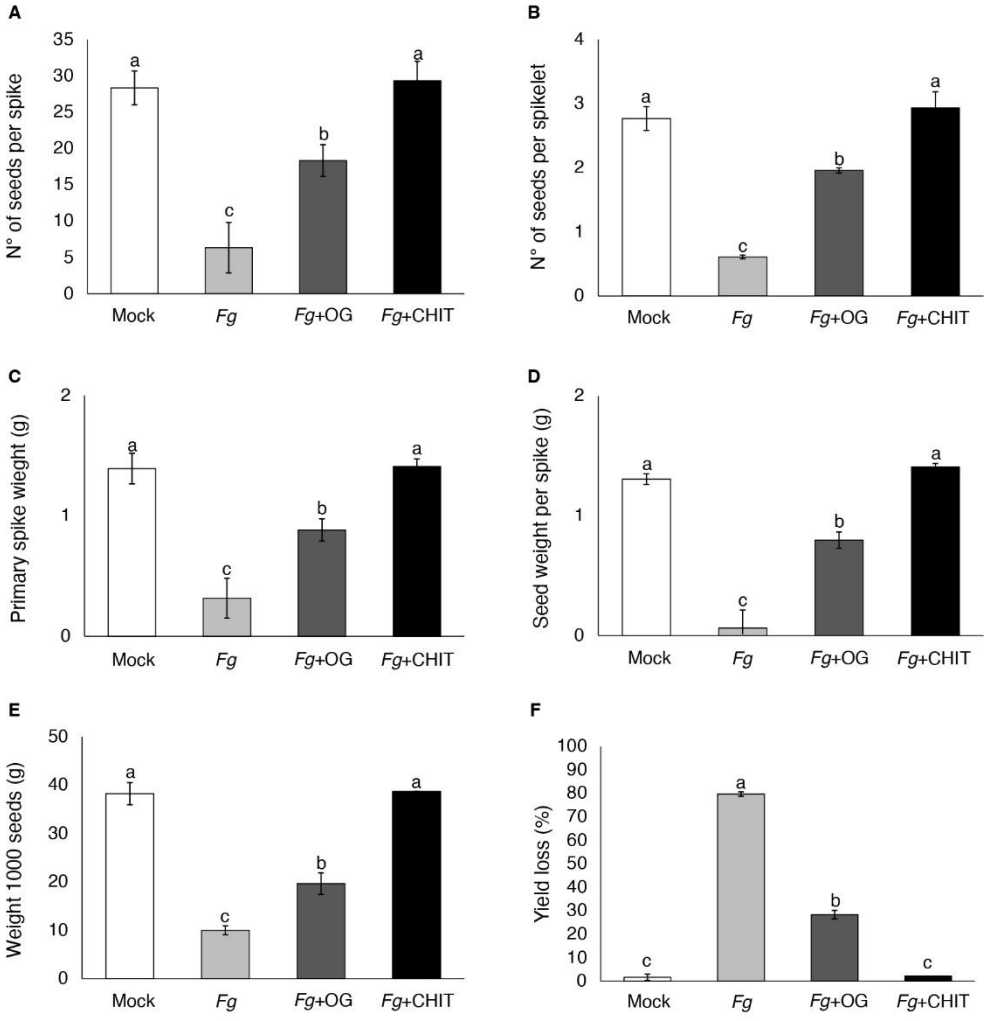

Figure 2. Agronomic and growth parameters in OG- and CHIT-cotreated wheat plants after *F. graminearum* infection. A) Number of seeds per spike; **B)** Number of seeds per spikelet; **C)** Primary spike weight (g); **D)** Seed weight per spike (g); **E)** Weight 1000 seeds (g); **F)** Yield loss (%) for the wheat cv. Svevo. A minimum of 10 plants per treatment condition were analyzed to obtain data. All values are the means ± standard error (SE). The statistical significance was tested by means of ANOVA followed by Tukey test. Different letters indicate statistically different values ($p < 0.05$).

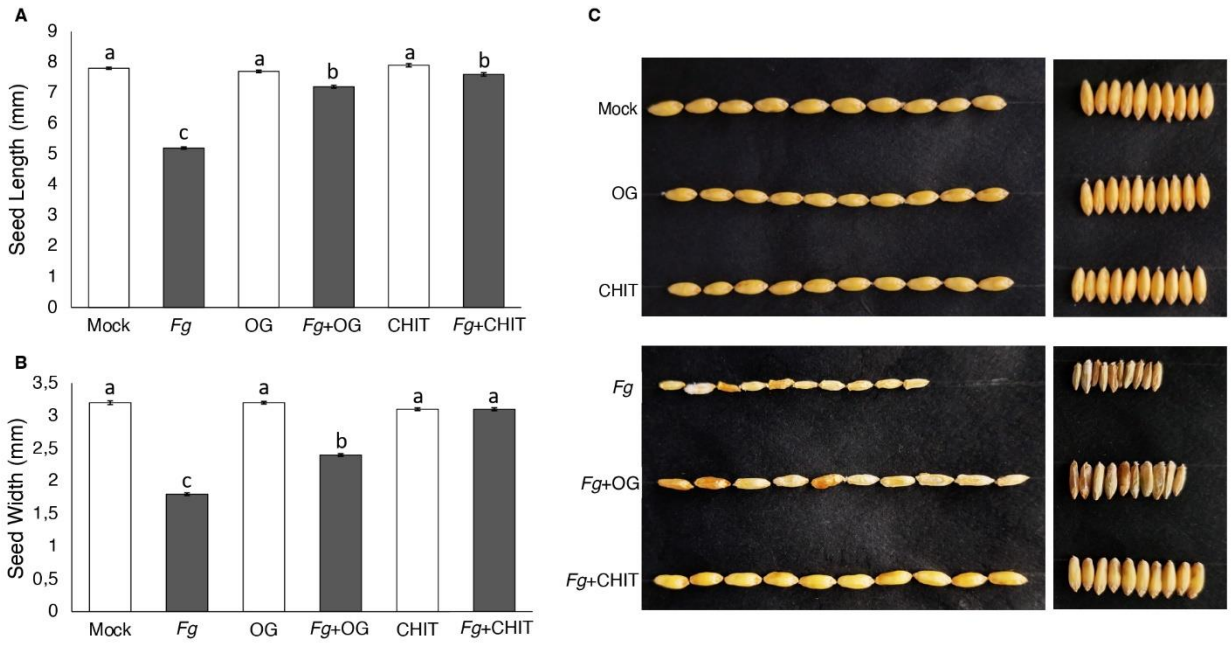

Figure 3. Seed quality and filling in OG- and CHIT-cotreated wheat plants after *F. graminearum* infection. A) Seed length (mm); **B)** Seed width (mm); **C)** Photographs showing length and width of representative seeds for each treatment condition. Ten seeds per treatment were analyzed to obtain data. All values are the means ± standard error (SE). The statistical significance was tested by means of ANOVA followed by Tukey test. Different letters indicate statistically different values ($p < 0.05$).

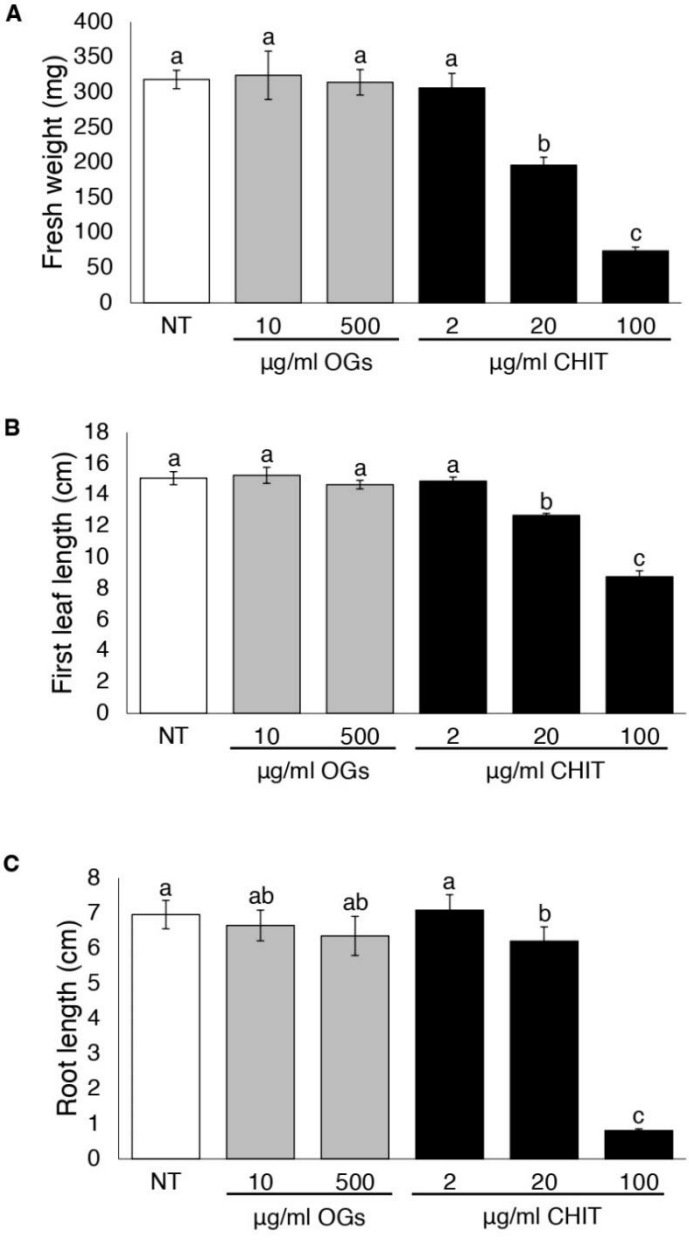

Figure 4. Effects on morphological parameters of wheat seedlings grown in MS medium in the absence or presence of different concentrations of purified OGs or CHIT. A) Fresh weight; **B)** Root length; **C)** First leaf length. The measurements were carried out 7 days after transplanting in MS medium. The statistical significance was tested by means of ANOVA followed by Tukey test. Different letters indicate statistically different values ($p < 0.05$).

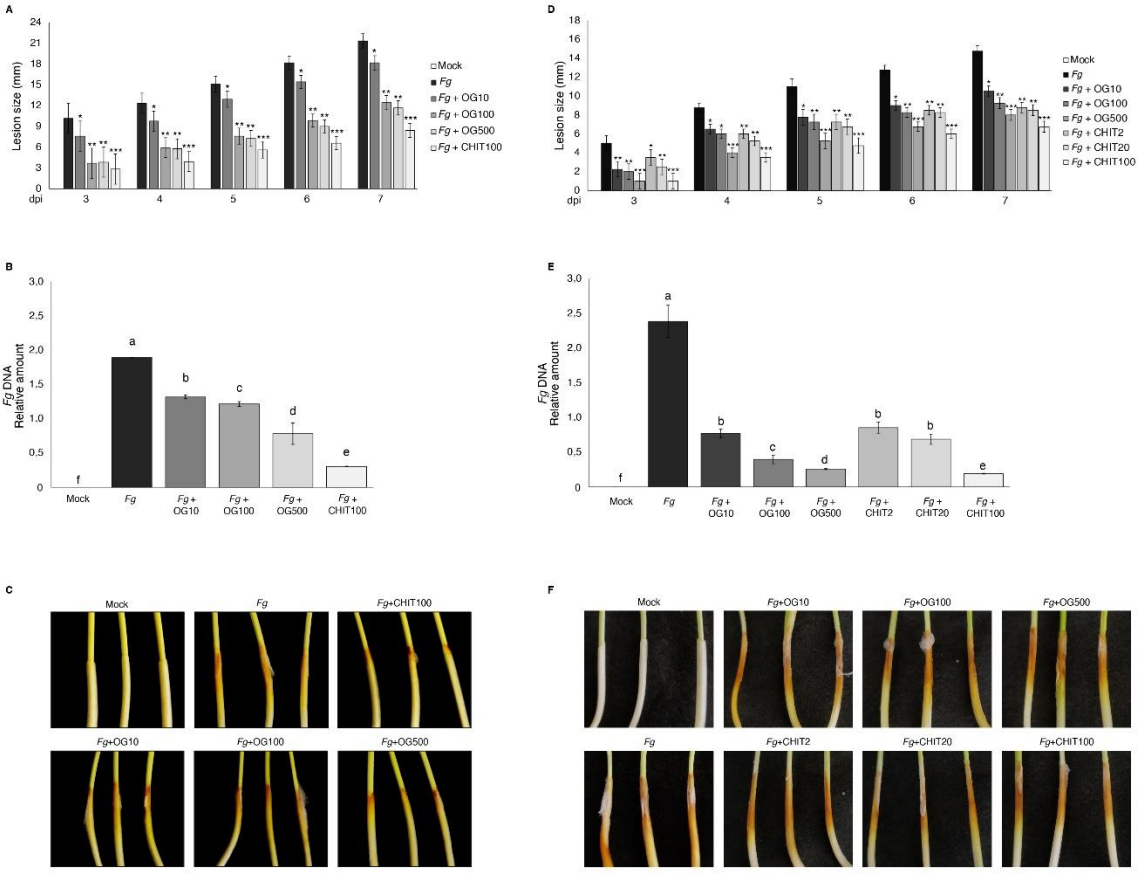

Figure 5. OGs trigger local and systemic resistance to FHB in a dose-dependent manner. Coleoptile lesion size in Svevo seedlings locally co-treated with *Fg*, *Fg*+OGs or *Fg*+CHIT (**A**) or grown in the absence or presence of the indicated amounts of elicitors for 3 days and then inoculated with *Fg* spores (**D**). Disease symptoms were monitored for 7 days post inoculation (dpi). **B** and **E)** Fungal genomic DNA quantification by real-time PCR analyses of the *Fgβ-tubulin* gene normalized to the wheat *TdACTIN* gene in wheat coleoptiles at 7 dpi; **C** and **F)** Images taken at 7 dpi showing disease spread in representative wheat coleoptiles for each treatment condition. All values are the means ± SE (n = 10). Asterisks above the bars indicate values that are significantly different from seedlings inoculated with the *Fg* alone (* $p < 0.05$, ** $p < 0.03$, *** $p < 0.01$, student t-test).

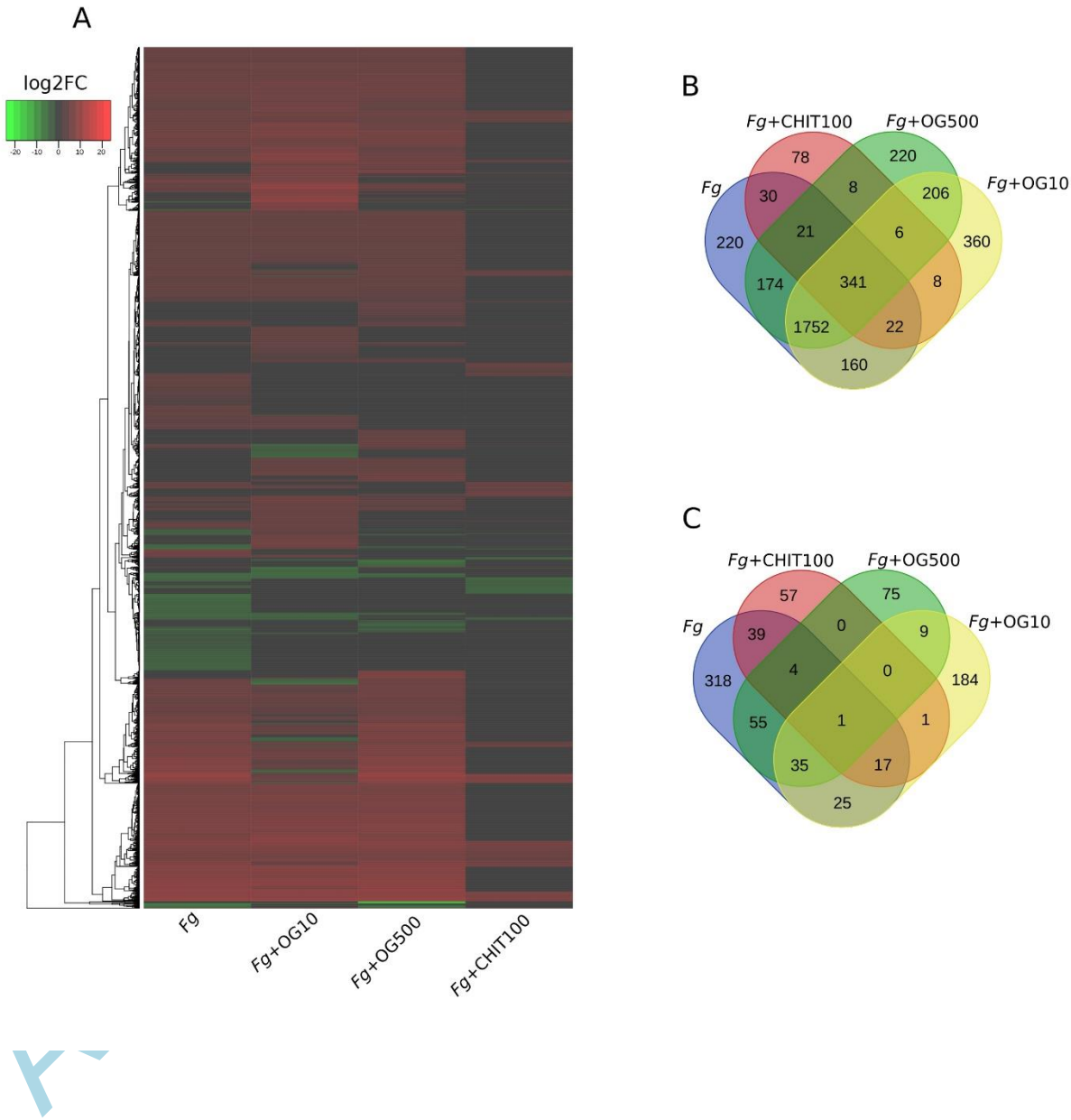

Figure 6. Heatmap and Venn diagrams depicting DEGs in the conditions *Fg*, *Fg*+OG10, *Fg*+OG500, *Fg*+CHIT100 *vs* control condition (mock). In (**A**), heatmap and hierarchical clustering of DEGs using the McQuitty algorithm. The heatmap shows the expression patterns of DEGs across four conditions compared to control one (mock), with red levels indicating up-regulated and green representing down-regulated DEGs. Different color intensity indicates different levels of expression (Log2Fold Change). In (**B**) and (**C**), Venn diagrams illustrate the overlap of up- and downregulated DEGs, respectively, between pairwise comparisons of the treatments.

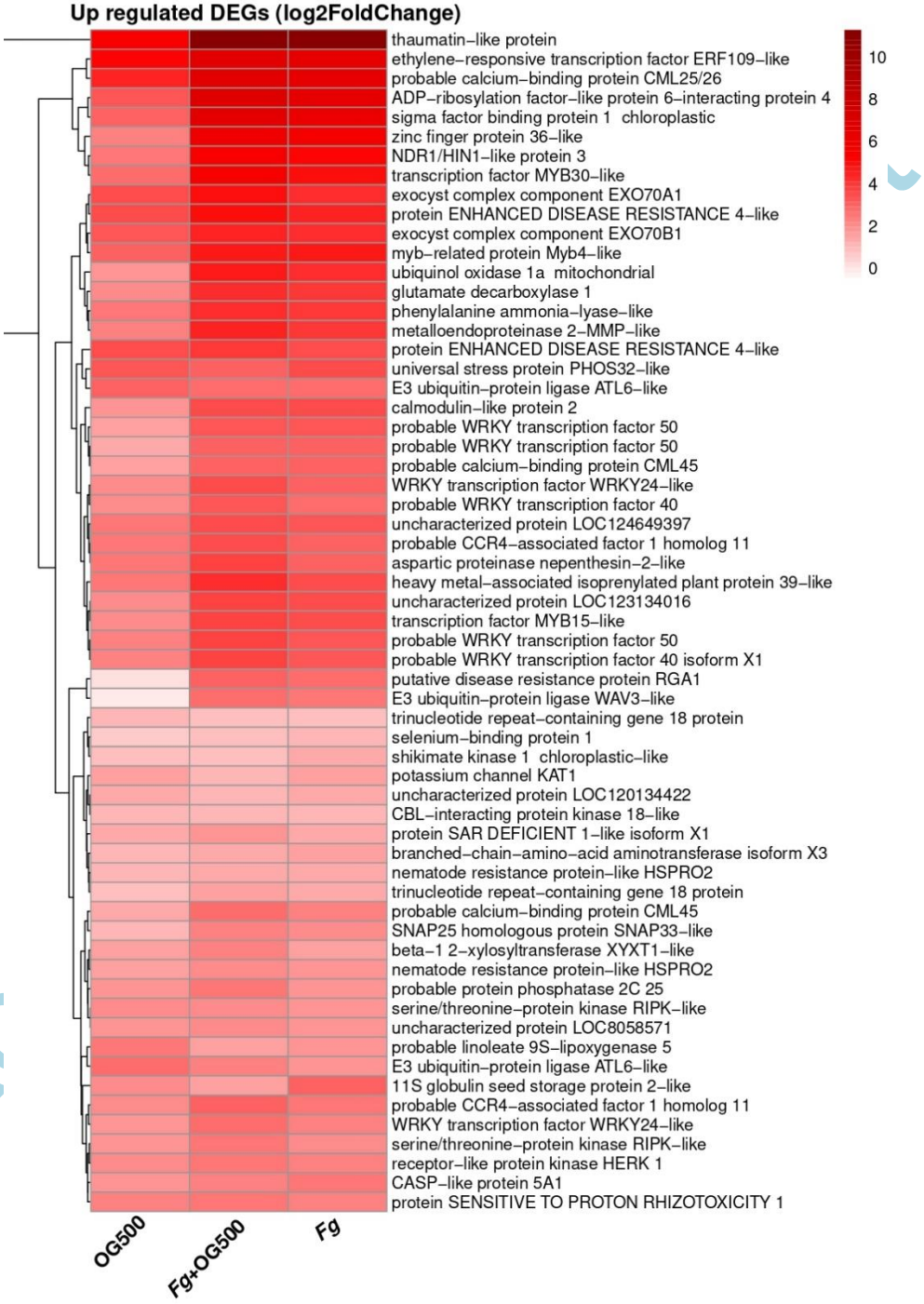

Figure 7. Heatmap depicting expression of 59 up-regulated DEGs shared by condition *Fg*, *Fg*+OG500 and OG500. These shared DEGs may be related to a common response mediated by *Fg* and OG 500 µg/ml. Different color intensity indicates different levels of expression (Log2Fold Change).

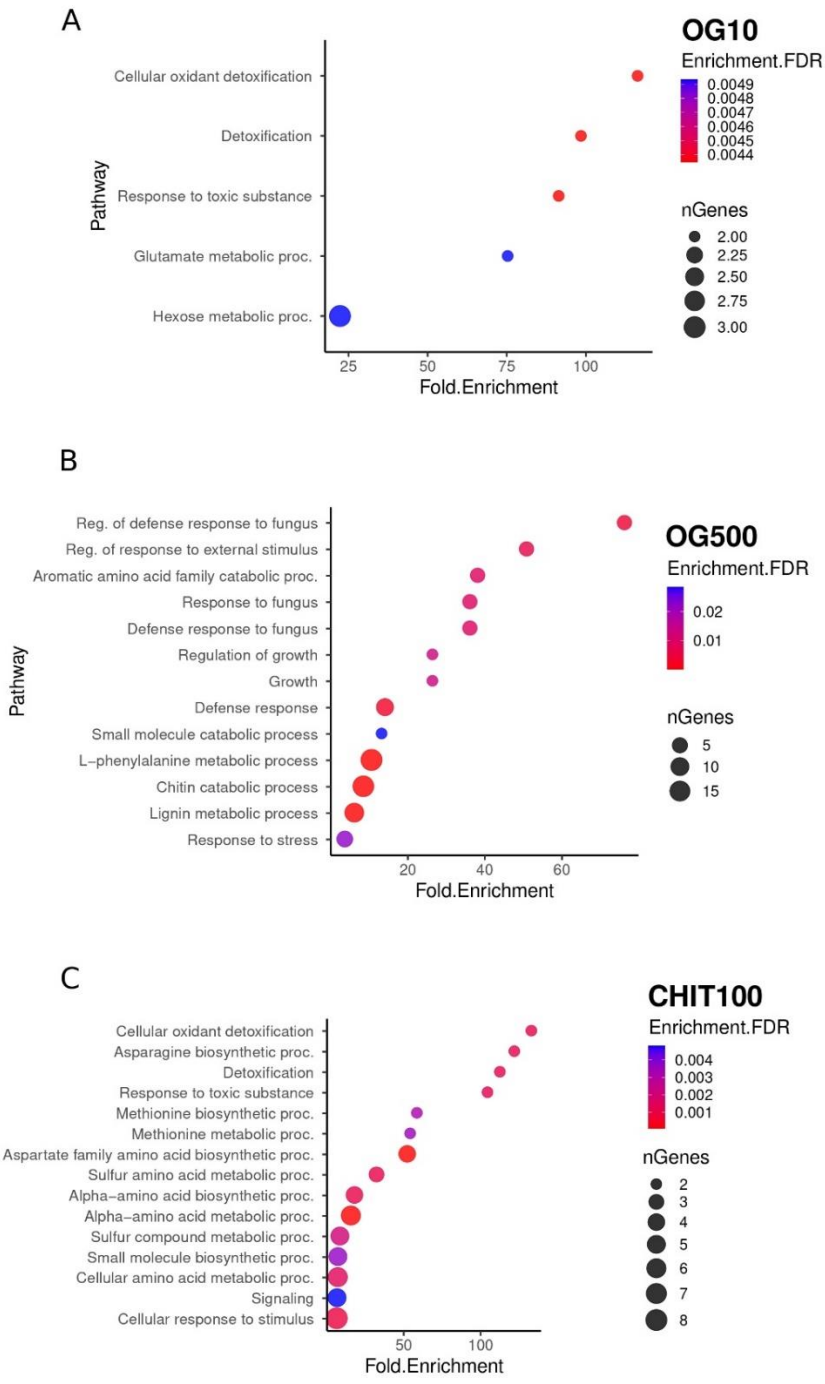

Figure 8. Bubble plots showing GO-enriched terms classified as Biological Process (BP) in detected DEGs. In detail, enriched terms in OG10 (**A**), OG500 (**B**), and CHIT100 (**C**) are reported. The x-axis shows the fold enrichment values, *i.e.*, the percentage of genes in the selected DEG list belonging to a pathway divided by the corresponding percentage in the all reference gene list, and the y-axis reports the GO terms. Sizes of bubbles are proportional to the number of genes assigned to the related GO term, while bubbles color indicates the significance of the enriched term (False Discovery Rate values) as calculated by the enrichment analysis by Blast2GO.

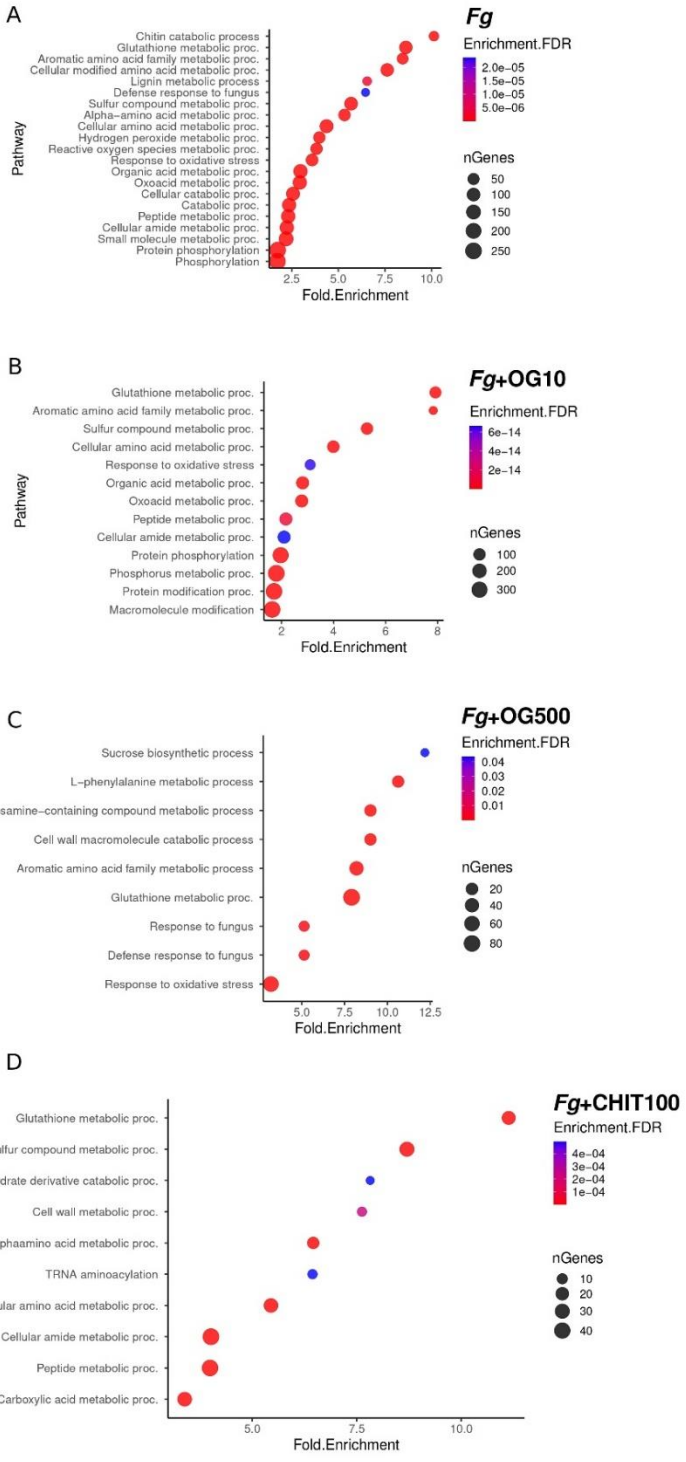

Figure 9. Bubble plots showing GO-enriched terms classified as Biological Process (BP) in detected DEGs. In detail, enriched terms in *Fg* (**A**), *Fg*+OG10 (**B**), *Fg*+OG500 (**C**), and *Fg*+CHIT100 (**D**), are reported. The x-axis shows the fold enrichment values, i.e. the percentage of genes in the selected DEG list belonging to a pathway divided by the corresponding percentage in the all reference gene list, and the y-axis reports the GO terms. Sizes of bubbles are proportional to the number of genes assigned to the related GO term, while bubbles color indicates the significance of the enriched term (False Discovery Rate values) as calculated by the enrichment analysis by Blast2GO.